

Thermalization in a simple spin-chain model

Peter Reimann and Christian Eidecker-Dunkel

Faculty of Physics, Bielefeld University, 33615 Bielefeld, Germany

(Dated: February 27, 2025)

We consider the common spin-1/2 XX-model in one dimension with open boundary conditions and a large but finite number of spins. The system is in thermal equilibrium at times $t < 0$, and is subject to a weak local perturbation (quantum quench) at $t = 0$. Focusing mainly on single-spin perturbations and observables, we show that the system re-thermalizes for sufficiently large times $t > 0$ without invoking any unproven assumptions besides the basic laws of quantum mechanics. Moreover, the time-dependent relaxation behavior is obtained in quantitative detail and is found to exhibit a wealth of interesting features.

I. INTRODUCTION

Thermalization in isolated many-body systems is a well-established empirical observation in numerous experiments and numerical investigations [1–4]. On the other hand, obtaining rigorous analytical results for some given model system is still considered as a very daunting task [5–8] if one admits no unproven assumption, postulate, or hypothesis besides the basic laws of quantum mechanics (see also Sec. II below). Here, we analytically show thermalization for a particularly simple model, namely the so-called XX-spin chain, after a weak local quantum quench. More precisely speaking, the system starts out in the canonical ensemble (Gibbs state) pertaining to some given pre-quench Hamiltonian, and then evolves under the action of a slightly (locally) perturbed post-quench Hamiltonian. Focusing mainly on single-spin perturbations, re-thermalization is shown in the sense that arbitrary single-spin observables (and arbitrary sums thereof) approach the canonical expectation values pertaining to the post-quench Hamiltonian for the vast majority of all sufficiently late times (after initial relaxation processes have died out).

Put differently, one arbitrary but fixed spin may be viewed as the subsystem of actual interest, and the entire rest of the chain as its environment (thermal bath). This subsystem is shown to (re-)thermalize after a small perturbation in the presence of the thermal bath.

Moreover, not only the long-time behavior, but also the entire time-dependent relaxation is analytically obtained and discussed. It exhibits a surprisingly rich structure, including some key features which have also been observed (but not analytically explained) before in many numerical explorations of more general models.

Technically, the main new ingredient is a rigorously provable generalization of Onsager’s regression hypothesis, recently obtained in Ref. [9]. Everything else in principle amounts to an application of standard methods, albeit the detailed calculations are quite involved and to our knowledge not readily available in the literature.

II. GENERAL FRAMEWORK

Consider an isolated many-body quantum system in a (pure or mixed) initial state $\rho(0)$, evolving under the action of some model Hamiltonian H according to von Neumann’s equation $i\dot{\rho}(t) = [H, \rho(t)]$ into the state

$$\rho(t) = e^{-iHt} \rho(0) e^{iHt} \quad (1)$$

in units with

$$\hbar = 1 . \quad (2)$$

The expectation value of any observable (Hermitian operator) A at time t is thus given by

$$\langle A \rangle_t := \text{tr}\{\rho(t)A\} . \quad (3)$$

Denoting the eigenvalues of H by E_n and the eigenvectors by $|n\rangle$, one readily finds that

$$\langle A \rangle_t = \sum_{mn} \rho_{mn}(0) A_{nm} e^{-i(E_m - E_n)t} , \quad (4)$$

where $\rho_{mn}(0) := \langle m|\rho(0)|n\rangle$ and $A_{nm} := \langle n|A|m\rangle$.

As usual, in cases where we are interested in a system in contact with some environmental bath, the Hamiltonian H is supposed to describe the (isolated) “supersystem” composed of the system of interest and the bath. Moreover, only special choices of A and $\rho(0)$ may then be of actual interest.

While Eq. (4) is still entirely general and exact, it is obvious that some additional knowledge about the quantities E_n , $\rho_{mn}(0)$, and A_{nm} is indispensable to admit any physically relevant conclusions.

For instance, one may try to show that the system exhibits the property of equilibration, meaning that the expectation values in Eq. (4) stay very close to some constant value (namely the long time-average of $\langle A \rangle_t$) for the vast majority of all sufficiently late times t . Rigorous proofs of such a behavior have been obtained for instance in Refs. [10–15] under certain (quite weak) assumptions regarding E_n , $\rho_{mn}(0)$, and A_{nm} . Most importantly, the energies E_n must not exhibit extremely high degeneracies. Similarly, extremely high degeneracies of the energy gaps $E_n - E_m$ must be excluded. Furthermore, the level populations $\rho_{nn}(0)$ (obeying $\rho_{nn}(0) \geq 0$

and $\sum_n \rho_{nn}(0) = 1$) must be very small for all n , apart from possibly one exceptional n . For systems with many degrees of freedom there are quite convincing physical arguments why those assumptions may be expected to be fulfilled in many cases, yet a rigorous analytical verification for a given model Hamiltonian and initial state is extremely difficult. Indeed, a rigorous demonstration of equilibration without any such physically reasonable but unproven extra assumptions has only been achieved very recently for some quite special models and observables (while the initial states may be rather general), see Refs. [5–8].

As a next step, one may take equilibration for granted and try to show that the system exhibits the property of thermalization, meaning that the long-time average of $\langle A \rangle_t$ is (approximately) equal to the thermal expectation value $\text{tr}\{\rho_{mc}A\}$, where ρ_{mc} is the pertinent microcanonical ensemble. This property can be verified for instance under the extra assumption that the so-called eigenstate thermalization hypothesis (ETH) is fulfilled [16–19] (see also [1–4]). However, until now the ETH has the status of a hypothesis, which to the best of our knowledge has not been rigorously derived for any (non-trivial) model Hamiltonian H and observable A . Alternative approaches to rigorously demonstrate thermalization for some given Hamiltonian and initial state have been devised for instance in Refs. [20, 21], however still utilizing (among others) some of the above mentioned unproven assumptions in the context of equilibration.

More precisely speaking, a given system (and initial state) is commonly regarded as exhibiting thermalization if every physically relevant observable does so [1–4]. Our first remark is that for any non-thermal initial state $\rho(0)$ there exist some Hermitian operators A which do not thermalize. Typically, these A involve projectors onto eigenstates of H and are usually viewed as being physically unrealistic (not experimentally feasible), at least for (reasonable) model systems with many degrees of freedom, as we consider them here. Therefore, the most commonly adopted standpoint is that only so-called local (i.e., short-ranged and few-body) operators A must be taken into account [1–4]. We also adopt this viewpoint in our present work. Note that thermalization then immediately follows also for arbitrary sums of local operators. Moreover, macroscopic observables of physical relevance are supposed to be always given by such sums of local operators, and are thus covered as well.

It is a long-known and commonly appreciated fact that integrable systems generally do not exhibit thermalization after a global quench, see for example Refs. [1–4, 22]. On the other hand, thermalization has been analytically proven in Refs. [5–8] for systems which are integrable and initial conditions which include global quenches as special cases. However, only some subset of observables has actually been addressed in these works, and there still must exist some other (physically relevant) observables, which do not thermalize [23].

Also in our present work, the considered models are

integrable, and hence are known to generally avoid thermalization after a *global* quench (see also Sec. IV B). This is the reason why we will only address *local* quenches. Furthermore, the number of degeneracies and degenerate energy gaps (see above) will turn out to increase exponentially with the system size. Hence, all the above-mentioned previous results [10–15] regarding the issue of equilibration will be useless in our present case.

On the other hand, in the definition of thermalization we will replace the microcanonical ensemble ρ_{mc} by the corresponding canonical ensemble

$$\rho_{can} := e^{-\beta H} / \text{tr}\{e^{-\beta H}\}, \quad (5)$$

$$\beta := 1/k_B T, \quad (6)$$

where T is the temperature and k_B Boltzmann’s constant, and where β is (as usual) chosen such that $\text{tr}\{\rho_{mc}H\} = \text{tr}\{\rho_{can}H\}$. In other words, we take for granted the equivalence of ensembles in the sense that $\text{tr}\{\rho_{mc}A\} = \text{tr}\{\rho_{can}A\}$ for all physically relevant observables A . A more rigorous justification of this equivalence is provided for instance in [24–27]. For the rest, this issue is not the actual main subject of our present paper. From an alternative viewpoint one could in fact employ ρ_{can} instead of ρ_{mc} already in the very definition of thermalization. The main reason is that in cases where the equivalence of the ensembles might be violated, it is not obvious which of them is the “right” one anyway (without invoking some unproven hypothesis such as Jaynes principle).

For further general remarks and comparisons with previous works we also refer to our Conclusions in Sec. VI.

III. SETUP

We focus on the XX-spin-chain model with open boundary conditions and Hamiltonian

$$H = -J \sum_{l=1}^{L-1} (s_{l+1}^x s_l^x + s_{l+1}^y s_l^y) - G \sum_{l=1}^L s_l^z, \quad (7)$$

where s_l^a with $a \in \{x, y, z\}$ are spin-1/2 operators at the chain sites $l \in \{1, \dots, L\}$, J quantifies the nearest neighbor interactions, and G the coupling to a homogeneous transverse field. Furthermore, we restrict ourselves to the non-trivial case $J \neq 0$, and we work in units such that the operators $2s_l^a$ can be represented as Pauli matrices in the eigenbasis of s_l^z (see also Eq. (2)).

It is well-known that this Hamiltonian can be analytically diagonalized by mapping it via a Jordan-Wigner transformation to an equivalent model of free (spinless) fermions. The details of this transformation are provided in Appendix A. Accordingly, such models are sometimes classified as noninteracting integrable systems in the recent literature [28]. Furthermore, the number of degeneracies and degenerate energy gaps of the Hamiltonian (7) can be shown to grow exponentially with the system

size L , see Appendix A 5. Yet another general property of this Hamiltonian is that it commutes with $S^z := \sum_{l=1}^L s_l^z$, i.e., S^z is a conserved quantity.

At time $t = 0$ the system is assumed to be in an initial state of the form

$$\rho(0) := e^{-\beta H_g} / \text{tr}\{e^{-\beta H_g}\}, \quad (8)$$

where

$$H_g := H - gV \quad (9)$$

is a slight modification of the original Hamiltonian from Eq. (7) with a local perturbation operator V and a coupling parameter g . While $\rho(0)$ in Eq. (8) thus amounts to a thermal equilibrium state (canonical ensemble) with respect to the modified Hamiltonian H_g , it is a non-equilibrium initial state with respect to the actual Hamiltonian H of the system we are considering, which then evolves for $t > 0$ according to Eq. (1), yielding time-dependent expectation values as defined in Eq. (3). Equivalently, these expectation values can be rewritten as

$$\langle A \rangle_t = \text{tr}\{\rho(0)A(t)\}, \quad (10)$$

where

$$A(t) := e^{iHt} A e^{-iHt} \quad (11)$$

is the observable at time t in the Heisenberg picture.

As discussed in Sec. II, the problem of thermalization then amounts to the question whether $\langle A \rangle_t$ stays sufficiently close to the thermal equilibrium value

$$A_{\text{th}} := \text{tr}\{\rho_{\text{can}} A\} \quad (12)$$

for the vast majority of all sufficiently late times t , where ρ_{can} is the canonical ensemble from Eq. (5). We remark that, in principle, the values of β in Eqs. (5) and (8) could still be different. But since we focus on local perturbations in Eq. (9) it is reasonable to expect, and will even be rigorously verified later on, that the values of β can indeed be chosen identical in our present case.

Similarly as in Eqs. (10)-(12), the temporal correlation (also called, among others, dynamic or two-point correlation function) of two Hermitian operators V and A at thermal equilibrium is defined as

$$C_{VA}(t) := \langle VA(t) \rangle_{\text{th}} - V_{\text{th}} A_{\text{th}}. \quad (13)$$

While V and A in this definition are still arbitrary, we henceforth always focus on the situation that V is the perturbation operator appearing in the initial condition (8) via Eq. (9), and A some local observable. (As already said in Sec. II, the extension to sums of such observables is immediate.) Under this premise we then can utilize the following result from [9],

$$\langle A \rangle_t - \langle A \rangle_{\text{th}} = g\beta \sum_{k=0}^{\infty} \frac{(i\beta)^k}{(k+1)!} \frac{d^k}{dt^k} C_{VA}(t), \quad (14)$$

connecting the time-dependent expectation values of a system out of equilibrium with the temporal correlations at thermal equilibrium.

Our first remark is that Eq. (14) is essentially a linear response kind of approximation in the sense that higher order corrections in $g\beta$ have been neglected on the right-hand side. More precisely speaking, it has been shown in Ref. [9] that the neglected terms can be upper bounded (in modulus) by $\|A\|_{\text{op}}(\epsilon^2 + \mathcal{O}(\epsilon^3))$, where $\|A\|_{\text{op}}$ is the operator norm of A (largest eigenvalue in modulus). Thus, we always may add a trivial constant to A in order to minimize $\|A\|_{\text{op}}$, and then utilize a trivial multiplicative factor so that $\|A\|_{\text{op}} = 1$. Furthermore,

$$\epsilon := g\beta \|V\|_{\text{op}} f_H(\beta), \quad (15)$$

where $f_H(\beta)$ depends on β and on the properties of the unperturbed system Hamiltonian H . For our specific model from Eq. (7), the function $f_H(\beta)$ turns out to be of order unity at least as long as the parameters βJ and βG are of order unity (or smaller). We thus can conclude that the approximation (14) will be very good if one of the two quantities β and $g\|V\|_{\text{op}}$ is sufficiently small. In particular, one of them may not be small if the other is all the smaller. Moreover, under the extra condition that βJ and βG are at most of order unity, it is sufficient that the product $g\beta\|V\|_{\text{op}}$ is small. Note that for extensive perturbations V , the operator norm $\|V\|_{\text{op}}$ generically diverges as the system size increases, hence our approximation (14) becomes questionable (it may still be valid, but there is not yet a proof). This is another reason (besides the one already mentioned above Eq. (5)) why we mainly focus on local perturbations in our present work. We finally emphasize that all these considerations regarding the accuracy of Eq. (14) are valid for arbitrary times t and chain-lengths L of the unperturbed system in Eq. (7).

Our second remark is that the correlations in Eq. (13) are in general complex-valued functions of t , and likewise for every single summand in Eq. (14). However, the entire sum can be shown to be real-valued [9], and hence every summand can be replaced by its real part. By keeping only the real part of the first summand (which equals Eq. (13)), one recovers the so-called Onsager regression hypothesis. While this hypothesis is well-known to become quantitatively incorrect beyond the classical limit, the main achievement of [9] is a rigorous derivation of the amended relation (14). Employing this relation plays a key role in our present work, since we will be able to exactly evaluate $C_{VA}(t)$ for a large class of operators V and A , while we did not succeed (even for our simple model in Eq. (7)) to directly evaluate the left-hand side of Eq. (14).

IV. MAIN EXAMPLES

As our first specific examples we consider perturbations V and observables A of the form

$$V = s_\nu^z, \quad A = s_\alpha^z \quad (16)$$

with arbitrary $\nu, \alpha \in \{1, \dots, L\}$. The systems's initial state is thus given by the canonical ensemble from Eqs. (8) and (9), where H is the XX-model from Eq. (7) and $V = s_\nu^z$, and this initial state then evolves in time according to Eq. (1). As detailed in Appendix C (which in turn is based on Appendices A and B), it is possible to evaluate the corresponding temporal correlations in Eq. (13) as well as the infinite sum on the right-hand side of Eq. (14) in closed analytical form without any further approximation, resulting in

$$\langle s_\alpha^z \rangle_t - \langle s_\alpha^z \rangle_{\text{th}} = g\beta \sum_{m,n=1}^L \tilde{S}_m^\nu \tilde{S}_n^\nu \tilde{S}_m^\alpha \tilde{S}_n^\alpha f_{mn} e_{mn}(t), \quad (17)$$

$$\tilde{S}_k^l := \sqrt{\frac{2}{L+1}} \sin(\pi kl / (L+1)), \quad (18)$$

$$f_{mn} := \frac{\tanh(\beta \tilde{E}_m / 2) - \tanh(\beta \tilde{E}_n / 2)}{2\beta(\tilde{E}_m - \tilde{E}_n)}, \quad (19)$$

$$e_{mn}(t) := e^{-i(\tilde{E}_m - \tilde{E}_n)t}, \quad (20)$$

$$\tilde{E}_k := -J \cos(\pi k / (L+1)) - G. \quad (21)$$

In other words, the only approximations in this result are those discussed around Eq. (15) (complemented by $\|A\|_{\text{op}} = \|V\|_{\text{op}} = 1/2$ according to Eq. (16), and working in units as specified below Eq. (7)). The purpose of the tilde symbols is to better distinguish, for instance, \tilde{E}_k from E_n (see above Eq. (4)), or \tilde{S}_k^l from s_i^a and S^z (see below Eq. (7)).

One readily verifies that the right-hand side of Eq. (17) is a real-valued function of t . Therefore, only the real part of $e_{mn}(t)$ in Eq. (20) actually contributes, and the result in Eq. (17) is time-inversion invariant.

As detailed in Appendix A, the quantities \tilde{S}_k^l in Eq. (18) are the elements of a unitary matrix (see Eq. (A48)), i.e., they satisfy the orthonormality relations

$$\sum_{\nu=1}^L \tilde{S}_m^\nu \tilde{S}_n^\nu = \delta_{mn}, \quad \sum_{n=1}^L \tilde{S}_n^\nu \tilde{S}_n^\alpha = \delta_{\nu\alpha}. \quad (22)$$

[Alternatively, one also may derive these relations directly from Eq. (18).] Concerning the quantities f_{mn} in Eq. (19) one can furthermore show that

$$0 < f_{mn} \leq 1/4 \quad \text{for all } m, n, \quad (23)$$

as detailed in Appendix D (see Eq. (D4) therein).

A first remarkable feature of Eq. (17) is the symmetry with respect to the indices ν and α , and thus with respect to the perturbation V and the observable A from Eq. (16). Second, the transverse field strength

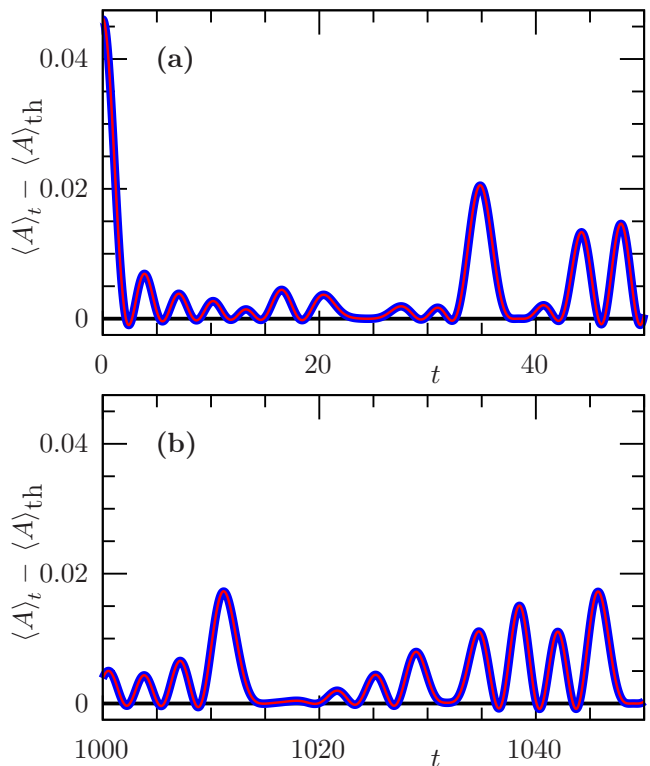


FIG. 1. Blue: Numerically exact results for the expectation values $\langle A \rangle_t - \langle A \rangle_{\text{th}}$, employing the XX-model from Eq. (7) with $L = 16$, $J = 1$, and $G = 0$, the perturbation V and observable A from Eq. (16) with $\nu = \alpha = L/2$, and the initial condition from Eqs. (8) and (9) with $\beta = 1$ and $g = 0.2$. Red: Corresponding analytical approximation from Eq. (17). (a): Initial relaxation behavior for $t \in [0, 50]$. (b): Long-time behavior for $t \in [1000, 1050]$. The differences between the red and blue curves are at most about 10^{-4} , and hence not visible on the scale of this plot.

G from Eq. (7) only enters into Eq. (17) via Eq. (19), while Eq. (20) is independent of G according to Eq. (21). Third, the number of summands in Eq. (17) grows only quadratically with the system size L , while such sums (for instance in Eq. (4)) are usually expected to grow exponentially with the system size. We speculate that this might possibly be due to our special (integrable noninteracting) model (see below Eq. (7)), or due to the fact that only linear order terms in $g\beta$ have been kept (see above Eq. (15)). Our last remark is that by summing over α in Eq. (17) and exploiting Eq. (22) one readily can infer that $S^z := \sum_{\alpha=1}^L s_\alpha^z$ is indeed a conserved quantity (see above Eq. (8)).

A further general symmetry property is based on the trivial identity

$$\sum_{n=1}^L c_n = \sum_{n=1}^L c_{L+1-n} \quad (24)$$

for arbitrary summands c_n . We thus may replace all indices n in Eq. (17) by $L+1-n$, and similarly for m .

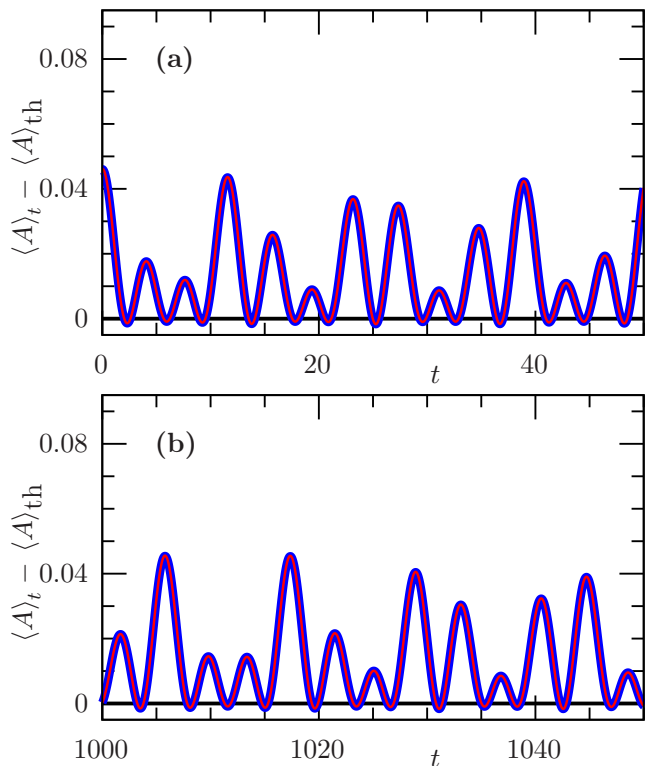


FIG. 2. Same as in Fig. 1 but for a smaller system with $L = 4$.

According to Eq. (18), this means that \tilde{S}_m^ν is replaced by $(-1)^{\nu+1}\tilde{S}_m^\nu$ and analogously for all the other factors in Eq. (17). Denoting the right-hand side of Eq. (17) as a function $F(\beta, J, G)$ of the three basic model parameters β , J , and G , one thus finds after some elementary calculations that $F(\beta, J, G) = F(\beta, J, -G)$. Recalling that only the real part of Eq. (20) actually counts (see below Eq. (21)) one furthermore can infer from Eq. (17) that $F(\beta, -J, -G) = F(\beta, J, G)$. Combining both findings yields $F(\beta, -J, G) = F(\beta, J, G)$. Finally, $F(-\beta, J, G) = -F(\beta, J, G)$ is immediately evident from Eq. (17). Altogether, we thus can conclude that Eq. (17) must be an odd function of β , and an even function of J and of G .

For the rest, the approximation (17) is still quite complicated from a purely analytical viewpoint, but can be easily evaluated numerically even for rather large chain-lengths L . On the other hand, a direct, numerically exact evaluation of the quantity on the left-hand side of Eq. (17) is practically only feasible by diagonalizing the full many-body Hamiltonian from Eq. (7), and is thus restricted to relatively small L -values. Fig. 1 exemplifies such numerically exact results (blue curves) together with the (numerically evaluated) approximation from Eq. (17) (red curves). The close agreement of the two curves indicates that the approximation is very accurate. Moreover, the agreement is very good not only with respect to the initial relaxation behavior in (a), but also for the very

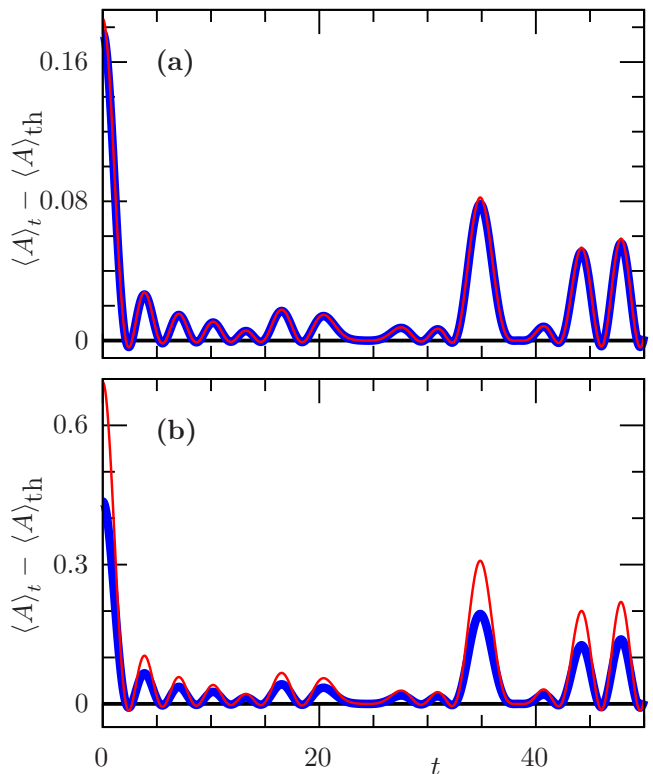


FIG. 3. Same as in Fig. 1 (a) but for stronger perturbations with $g = 0.8$ in (a) and $g = 3.0$ in (b). The differences between the blue and red curves are still quite small in (a), but clearly visible in (b).

late times in (b), as predicted below Eq. (15). Likewise, Fig. 2 illustrates the prediction below Eq. (15) that the approximation works equally well for a short chain with $L = 4$ as for the longer chain with $L = 16$ in Fig. 1.

While the differences between the exact (blue) and approximative (red) curves are hardly visible in Figs. 1 and 2, larger values of g have been chosen in Fig. 3 in order to better visualize the higher order corrections in g , which have been neglected in the approximation (17), see also the discussion around Eq. (15). Incidentally, one can show by symmetry arguments [29] that the left-hand side of Eq. (17) must be an odd function of the parameter g provided that $G = 0$. Hence, the neglected terms on the right-hand side of the approximation (17) must be (at least) of order g^3 . Fig. 3 shows a direct comparison between a numerically exact evaluation of the quantity on the left-hand side of Eq. (17) (blue) and its approximation as given by the right-hand side of Eq. (17) (red). A closer inspection of Fig. 3 shows that the differences between the two curves are indeed in good agreement with this prediction that they should grow as g^3 .

Finally, Fig. 4 illustrates the analogous finite- β effects. Our first remark is that we adopted in Fig. 4 the same, relatively large perturbation strength $g = 0.8$ as in Fig. 3 (a) in order to obtain clearly visible differences between the blue and red curves. Our second remark is that

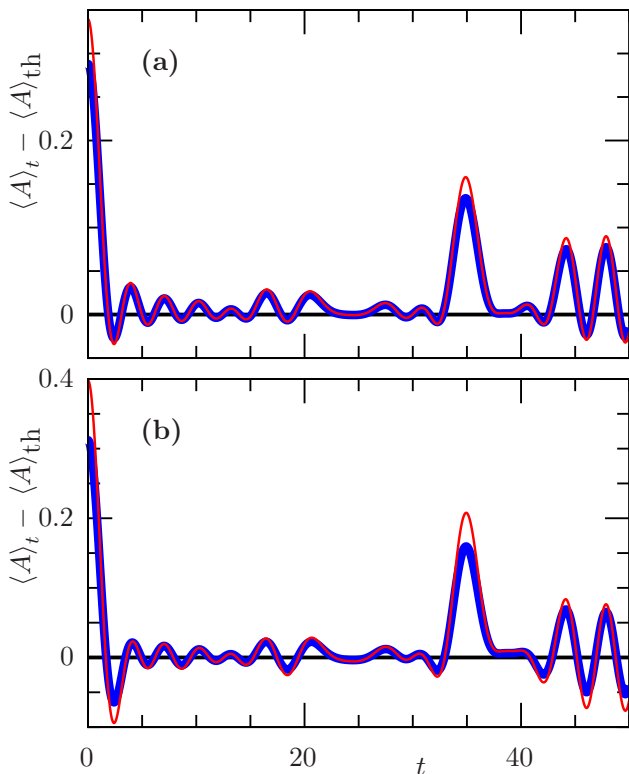


FIG. 4. Same as in Fig. 3 (a) but for larger β -values (smaller temperatures, see also Eq. (6) and main text), namely $\beta = 2$ in (a) and $\beta = 4$ in (b).

the curves in Fig. 4 (b) were found to hardly change any more upon further increasing β , i.e., we are already close to the zero temperature asymptotics for our present, still relatively small system with $L = 16$. Our last remark is that the relative differences between the red and blue curves both in Figs. 3 and 4 seem to be approximately independent of t , but we did not succeed to come up with an analytical explanation of this numerical observation.

We believe that further numerical illustrations that the approximation (17) indeed works very well also for other values of G in Eq. (7) and of ν and α in Eq. (16) may not be indispensable at this point. Henceforth, we will thus take Eq. (17) for granted, and we will focus on a more detailed discussion of the complicated expression on the right-hand side. Furthermore, in our subsequent plots of Eq. (17) we can and will remove the dependence on g by dividing both sides by g . (Incidentally, the dependence of Eq. (17) on β is far less trivial, see also Fig. 4). We finally remark that also the thermal expectation values $\langle s_\alpha^z \rangle_{\text{th}}$ appearing in Eq. (17) can be analytically evaluated (without any approximation) and discussed analogously to the right-hand side of Eq. (17), as detailed in Appendix E.

A. Proof of thermalization

This section is devoted to the derivation of thermalization as one of the key results of our paper. We proceed as follows. Taking the approximation (17) for granted, we will show in a first step that its long-time average becomes arbitrarily small for sufficiently large system sizes L (thermodynamic limit). In a second step we show that an analogous property also applies to the corresponding temporal mean square fluctuations. Finally, we explain why these two findings imply the property of thermalization as specified in detail in Sec. II.

To begin with, we rewrite Eq. (17) as

$$\langle s_\alpha^z \rangle_t - \langle s_\alpha^z \rangle_{\text{th}} = \sum_{m,n=1}^L K_{mn}^{\nu\alpha} e^{iE_{nm}t}, \quad (25)$$

where

$$K_{mn}^{\nu\alpha} := g\beta \tilde{S}_m^\nu \tilde{S}_n^\nu \tilde{S}_m^\alpha \tilde{S}_n^\alpha f_{mn}, \quad (26)$$

$$E_{nm} := \tilde{E}_n - \tilde{E}_m. \quad (27)$$

From Eq. (21) one can infer that $\tilde{E}_n \neq \tilde{E}_m$ for all $n, m \in \{1, \dots, L\}$ with $n \neq m$ (assuming $J \neq 0$, see below Eq. (7)). Denoting the long-time average by an overline symbol, we thus can conclude that

$$\overline{e^{iE_{nm}t}} = \delta_{nm}. \quad (28)$$

Together with Eqs. (25)-(27) it follows that

$$\overline{\langle s_\alpha^z \rangle_t} - \langle s_\alpha^z \rangle_{\text{th}} = g\beta \sum_{n=1}^L (\tilde{S}_n^\nu \tilde{S}_n^\alpha)^2 f_{nn}. \quad (29)$$

Exploiting Eqs. (18) and (23) we can conclude that $0 \leq (\tilde{S}_n^\nu \tilde{S}_n^\alpha)^2 f_{nn} \leq 1/L^2$ and thus

$$0 \leq \overline{\langle s_\alpha^z \rangle_t} - \langle s_\alpha^z \rangle_{\text{th}} \leq g\beta/L \quad \text{if } g\beta \geq 0. \quad (30)$$

Hence, the long-time average $\overline{\langle s_\alpha^z \rangle_t}$ must approach the thermal equilibrium value $\langle s_\alpha^z \rangle_{\text{th}}$ from above as the system size L increases. Analogous conclusions apply if $g\beta < 0$.

Next we turn to the temporal variance (or mean square fluctuations)

$$\sigma^2 := \overline{\left(\langle s_\alpha^z \rangle_t - \overline{\langle s_\alpha^z \rangle_t} \right)^2}. \quad (31)$$

Observing that $\langle s_\alpha^z \rangle_t - \overline{\langle s_\alpha^z \rangle_t}$ in Eq. (31) is equal to the difference between Eq. (25) and Eq. (29), it follows that

$$\sigma^2 = \overline{\left(\sum_{m \neq n} K_{mn}^{\nu\alpha} e^{iE_{nm}t} \right)^2} \leq \overline{\left(\sum_{mn} K_{mn}^{\nu\alpha} e^{iE_{nm}t} \right)^2}, \quad (32)$$

where the first sum runs over all $m, n \in \{1, \dots, L\}$ with $m \neq n$ and the second sum over all $m, n \in \{1, \dots, L\}$. Finally, this implies

$$\sigma^2 \leq \sum_{mn} \sum_{jk} K_{mn}^{\nu\alpha} K_{jk}^{\nu\alpha} \overline{e^{i(E_{nm} - E_{jk})t}}. \quad (33)$$

Similarly as below Eq. (29) one can show that $|K_{mn}^{\nu\alpha}| \leq |g\beta|/L^2$, and with Eq. (33) that

$$\sigma^2 \leq (g\beta)^2 \gamma / L, \quad (34)$$

$$\gamma := \frac{1}{L^3} \sum_{mnj} \sum_k \left| e^{i(E_{nm} - E_{jk})t} \right|. \quad (35)$$

Similarly as in Eq. (28), the summands in Eq. (35) are unity whenever $E_{nm} = E_{jk}$ and zero otherwise. According to Eq. (27), the latter criterion is equivalent to

$$\tilde{E}_m - \tilde{E}_n + \tilde{E}_j = \tilde{E}_k. \quad (36)$$

Let us temporarily consider m, n, j as arbitrary but fixed. Since \tilde{E}_k is a strictly monotonic function of k according to Eq. (21), it follows that there is at most one k for which Eq. (36) is fulfilled. As a consequence, the innermost sum over k in Eq. (35) can be upper bounded by unity, and thus the remaining triple sum over n, m, j by L^3 , implying

$$0 \leq \gamma \leq 1. \quad (37)$$

It follows that σ^2 in Eq. (34) approaches zero as the system size L increases. In view of Eq. (31) we can conclude that $\langle s_\alpha^z \rangle_t$ must be close to $\overline{\langle s_\alpha^z \rangle}_t$ for the vast majority of all times t . In turn, $\langle s_\alpha^z \rangle_t$ approaches the thermal equilibrium value $\langle s_\alpha^z \rangle_{\text{th}}$ for large L , see below Eq. (30). Altogether, the system thus exhibits thermalization (at least as far as the observables $A = s_\alpha^z$ from Eq. (16) are concerned, see also Secs. II and V). A more detailed discussion of this issue is postponed to the next subsection.

Incidentally, it seems reasonable to expect that for any given pair m, n the number of pairs j, k with the property $E_{nm} = E_{jk}$ is non-extensive in the system size L . This implies that γ in Eq. (35) decreases as $1/L$ and thus σ^2 in Eq. (34) as $1/L^2$. However, a rigorous derivation of such a stronger bound (compared to Eq. (37)) is not obvious, and therefore not further pursued here.

1. Discussion

Fig. 5 exemplifies these predictions in quantitative detail. In particular, Fig. 5 (b) provides convincing evidence that the long-time average approaches the thermal equilibrium value from above like $1/L$, in agreement with Eq. (30). Moreover, Fig. 5 (b) also provides reasonably good evidence that the time-averaged variance σ^2 from Eq. (31) scales as $1/L^2$ (actually, the evidence is that the dispersion σ scales as $1/L$), as heuristically predicted in the previous paragraph, and of course also in agreement with Eqs. (34), (37).

Note that the right-hand side of Eq. (17) is a quasi-periodic function of t , meaning that there must exist time-points t at which the expectation value returns arbitrarily close to its initial value (quantum recurrences). Likewise, there must exist even more frequent temporal

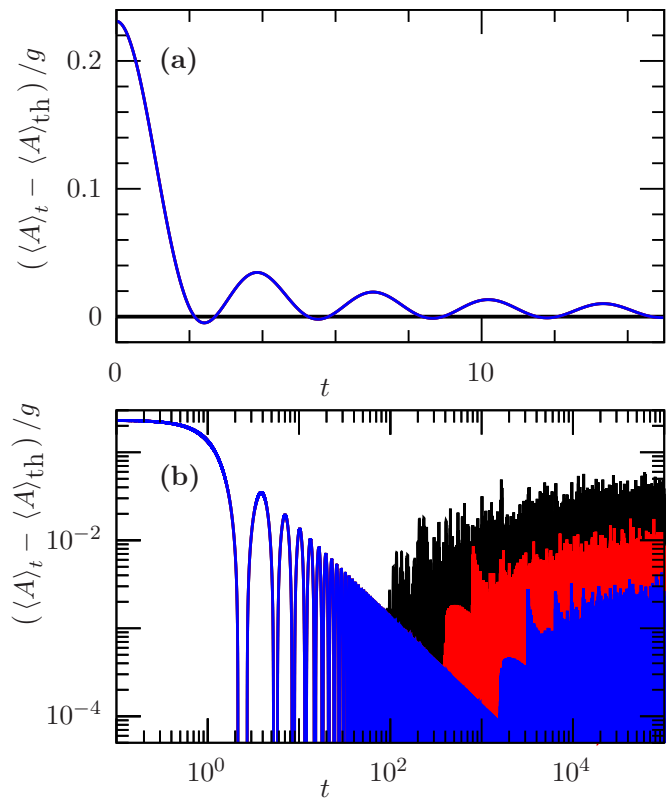


FIG. 5. (a) Numerical evaluation of Eq. (17) divided by g for $L = 100$ (black), $L = 400$ (red), $L = 1600$ (blue). Everything else as in Fig. 1. (b) Same data but now plotted double-logarithmically. Up to $t \approx 100$ the black curves are covered by the blue ones, and likewise for the red curves up to $t \approx 400$.

“fluctuations” which are smaller than those corresponding to such recurrences, but which are still non-negligible (experimentally observable). Only those are actually visible in Fig. 5 (b), since “true” recurrences are way too rare to be observable on this time scale (for the much smaller system in Fig. 2, some of the fluctuations already come close to “true” recurrences). Eqs. (34), (37) predict, and Fig. 5 (b) numerically illustrates that all the non-negligible deviations from the thermal expectation value become more and more rare as the system size increases, and provided one disregards the initial relaxation phase. (The latter is in some sense quite similar to one of the above-mentioned recurrences.) It is well-known that qualitatively, all these features also arise in more general many-body systems via Eq. (4). But to the best of our knowledge, our present theory (17) captures them for the first time analytically in full quantitative detail.

A further interesting feature of Fig. 5 (b) is the fact that the above-mentioned temporal fluctuations are practically invisible up to times t of the order of L (in our present units). Put differently, the detailed t -dependence for $t \leq \mathcal{O}(L)$ remains (practically) unchanged upon further increasing L (even in the limit $L \rightarrow \infty$), while the “fluctuations” for $t \geq \mathcal{O}(L)$ still exhibit quite significant pseudo-random changes upon increasing L . A similar be-

havior has been often seen before in numerical studies, while our analytical result (17) represents the first quantitative explanation we know of. Qualitatively, the usual heuristic argument is [30–34] that up to times until which the “signal” of our quantum quench at site ν (see Eqs. (9) and (16)) had sufficient time to reach both chain ends, the system cannot “know” that the distance between the ends is finite, hence it behaves (nearly) as if the ends were infinitely far apart. Assuming that the signal speed can be estimated by the pertinent Lieb-Robinson bound, it follows that the time in question increases linearly with the system size. Once again, this general heuristic argument is nicely reproduced by our analytical finding (17) according to Fig. 5 (b). For additional analytical insight we also refer to Sec. IV C 1.

Yet another, even more subtle feature which has often been observed in previous numerical investigations can also be seen in our present example in Fig. 5 (b): Near $t = L$, where the almost L -independent behavior goes over into the strongly L -dependent “fluctuations”, each curve seems to exhibit a minimum (on a slightly coarse-grained scale, or after taking some suitable running-time average). In other words, the system transiently appears to be closer to thermal equilibrium than at even later times. In hindsight, the same phenomenon can actually be observed already in Figs. 1, 3, and 4: Up to $t \simeq L = 16$, the oscillations appear to steadily die out, but later on they again become notably stronger. While this apparently very common phenomenon must be buried in Eq. (17), we did not succeed in pinning it down by purely analytical means.

B. Non-thermalization after a global quench

As mentioned in Sec. II, it is commonly expected [1–4, 22] that our present (integrable) model from Eq. (7) generically does not exhibit thermalization after a global quench. A particular example of this kind arises if the perturbation operator V in Eq. (9) is chosen as

$$V = \sum_{\nu=1}^L s_{\nu}^z . \quad (38)$$

Though the approximation (14) has not yet been rigorously justified in such a case (see also the discussion below Eq. (15)), it seems reasonable to conjecture that the effects of weak perturbations are additive. If so, we simply have to add up the effects of the single s_{ν}^z 's in Eq. (16) to obtain the pertinent results for our present perturbation in Eq. (38). Upon summing over all $\nu = 1, \dots, L$ in Eq. (17) and exploiting Eqs. (20), (22) one thus obtains

$$\langle s_{\alpha}^z \rangle_t - \langle s_{\alpha}^z \rangle_{\text{th}} = g\beta \sum_{n=1}^L (\tilde{S}_n^{\alpha})^2 f_{nn} \quad (39)$$

independent of t . Focusing on cases with $|\beta J| \ll 1$, the quantities f_{nn} can furthermore be approximated by

$1/[4 \cosh^2(\beta G/2)]$, as shown in Appendix D (see Eq. (D8) therein). Together with Eqs. (22) and (39) this yields

$$\langle s_{\alpha}^z \rangle_t - \langle s_{\alpha}^z \rangle_{\text{th}} = \frac{g\beta}{4 \cosh^2(\beta G/2)} . \quad (40)$$

Similarly as in the previous subsection we thus can conclude that the system indeed does *not* exhibit thermalization.

The specific perturbation V from Eq. (38) has the advantage of being easily tractable and the shortcoming that Eq. (39) is time-independent. For more general perturbations which consist of an extensive sum of single spins s_{ν}^z , it is reasonable to expect a generally non-trivial time-dependence of $\langle s_{\alpha}^z \rangle_t - \langle s_{\alpha}^z \rangle_{\text{th}}$. By similar arguments as below Eqs. (29) and (38), one moreover expects that $\langle s_{\alpha}^z \rangle_t - \langle s_{\alpha}^z \rangle_{\text{th}}$ still approaches a non-vanishing value for large L , which is again sufficient to rule out thermalization.

We reiterate that we employed an unproven (albeit reasonable) conjecture below Eq. (38).

As mentioned below Eq. (12), one might furthermore object that thermalization may possibly still occur if two different values of β in Eqs. (5) and (8) are chosen (but the two values still must be independent of the considered observable).

In conclusion, our above line of reasoning is far from a rigorous demonstration of non-thermalization after a global quench, but it shows that our present approach is at least not in contradiction to this widespread expectation [1–4, 22].

C. Approximation for long chains

We begin by explaining the main ideas for a particularly simple special case. Namely, we assume that

$$|\beta J| \ll 1 . \quad (41)$$

As detailed in Appendix D (see Eq. (D8) therein), we thus can employ the approximation

$$f_{mn} \simeq \frac{1}{4 \cosh^2(\beta G/2)} =: \eta \quad (42)$$

for all m, n . Hence, Eq. (17) can be rewritten in the much simpler form

$$\langle s_{\alpha}^z \rangle_t - \langle s_{\alpha}^z \rangle_{\text{th}} = g\beta\eta |W(t)|^2 , \quad (43)$$

$$W(t) := \sum_{n=1}^L \tilde{S}_n^{\nu} \tilde{S}_n^{\alpha} e^{-i\tilde{E}_n t} . \quad (44)$$

Next we recall the symmetry under a sign change of J and/or of G as established below Eq. (24). Therefore, we can and will henceforth replace J by $|J|$ and G by $|G|$. Exploiting Eqs. (18), (21), and the identity

$$\sin(x) \sin(y) = [\cos(x - y) - \cos(x + y)]/2 , \quad (45)$$

it then follows from Eq. (44) that

$$W(t) = e^{i|G|t} \left[\tilde{W}_{|\nu-\alpha|}(\omega t) - \tilde{W}_{\nu+\alpha}(\omega t) \right], \quad (46)$$

where

$$\omega := |J| \quad (47)$$

and

$$\tilde{W}_k(t) := \frac{1}{L+1} \sum_{n=1}^L \cos\left(\frac{\pi kn}{L+1}\right) \exp\left\{it \cos\left(\frac{\pi n}{L+1}\right)\right\}. \quad (48)$$

For large values of L one thus obtains the asymptotic approximation

$$\tilde{W}_k(t) = \frac{1}{\pi} \int_0^\pi dx \cos(kx) \exp\{it \cos(x)\}. \quad (49)$$

The right-hand side can be readily related to one of the various integral representations of the Bessel functions of the first kind $J_k(t)$ (see for instance Eq. (9.1.21) in [37]), yielding

$$\tilde{W}_k(t) = i^k J_k(t). \quad (50)$$

Our approximation of Eq. (48) by Eq. (49) is justified if the summands in Eq. (48) change very little upon increasing n by unity. The same requirement must apply to each of the two factors under the sum in Eq. (48), i.e., the two conditions $k/L \ll 1$ and $t/L \ll 1$ must be satisfied. In order to employ the approximation (49) in Eq. (46) we therefore must require that

$$\omega t \ll L \quad (51)$$

and

$$\nu + \alpha \ll L. \quad (52)$$

Note that we also must require that $|\nu - \alpha| \ll L$, but this condition automatically follows from Eq. (52) and the fact that $\nu, \alpha \geq 1$ in Eq. (16). Likewise, our assumption $L \gg 1$ above Eq. (49) is automatically guaranteed by Eq. (52).

Given that Eqs. (41), (51), and (52) are fulfilled, we finally can infer from Eq. (43), (46), (50), and the general identity $|\nu - \alpha| = \nu + \alpha - 2 \min\{\nu, \alpha\}$ the approximation

$$\begin{aligned} \langle s_\alpha^z \rangle_t - \langle s_\alpha^z \rangle_{\text{th}} &= g\beta\eta \left[J_{|\nu-\alpha|}(\omega t) - \tau_\nu^\alpha J_{\nu+\alpha}(\omega t) \right]^2, \quad (53) \\ \tau_\nu^\alpha &:= (-1)^{\min\{\nu, \alpha\}}. \quad (54) \end{aligned}$$

Moreover, it is reasonable to expect that this approximation will become asymptotically exact for $L \rightarrow \infty$ (while keeping t , ν , and α fixed).

More precisely speaking, for any given (large but finite) L , our approximation (49) and all our subsequent conclusions will only apply up to moderately large times such that Eq. (51) is still fulfilled. Most notably, they no longer depend explicitly on L , only implicitly via the

validity condition (51). For even larger times than in Eq. (51), we have to recourse to the original result in Eq. (17) (or in Eq. (43)). All this is closely related to and in agreement with the discussion in Sec. IV A 1.

The asymptotic behavior of Eq. (53) for small and large times can be inferred from the well-known properties of the Bessel functions $J_k(t)$, which we collected for the sake of convenience in Appendix F. One thus obtains the approximations

$$\langle s_\alpha^z \rangle_t - \langle s_\alpha^z \rangle_{\text{th}} = g\beta\eta (\omega t/2)^{2|\nu-\alpha|} \quad (55)$$

for small t and

$$\langle s_\alpha^z \rangle_t - \langle s_\alpha^z \rangle_{\text{th}} = \frac{8g\beta\eta\nu^2\alpha^2}{\pi} \frac{\sin^2(\omega t \pm \pi/4)}{(\omega t)^3} \quad (56)$$

for large t , where the plus sign applies if $\nu - \alpha$ is odd, and the minus sign otherwise. More precisely speaking, Eq. (55) requires $\omega t \ll 1$ (see also Eq. (F1)), while Eq. (56) requires Eq. (51) (see also previous paragraph). Moreover, $\omega t \gg |(d-1/4)(d-9/4)|$ with $d := (\nu - \alpha)^2$ (see below Eq. (F9)) is known to be yet another sufficient (but possibly not necessary) prerequisite for the approximation of Eq. (53) by Eq. (56).

In view of Eq. (16), the condition (52) implies that both the perturbation and the observable are located close to the left chain-end. By symmetry, analogous results can be readily obtained if they are located near the right chain-end.

Next we turn to cases where the perturbation and the observable are not located near one of the chain ends. For instance, both may be located near the middle of the chain. More generally, let us assume instead of Eq. (52) that [38]

$$|\nu - \alpha| + 1 \ll L, \quad (57)$$

and that $\nu + \alpha$ increases with L in such a way that $(\nu + \alpha)/L$ is neither close to 0 nor to 2. It follows that the approximation of Eq. (48) by Eq. (49) is only justified for the first function $\tilde{W}_{|\nu-\alpha|}(\omega t)$ on the right-hand side of Eq. (46). On the other hand, it is now reasonable to expect that the second function $\tilde{W}_{\nu+\alpha}(\omega t)$ can be approximately neglected in view of the fact that the first cosine term on the right-hand side of Eq. (48) exhibits relatively fast oscillations as a function of the summation index n compared to the much slower variations of the second cosine term (see also Eq. (51)). Hence, the right-hand side of Eq. (48) approaches zero for large L . Exploiting Eq. (50), this yields the approximation

$$\langle s_\alpha^z \rangle_t - \langle s_\alpha^z \rangle_{\text{th}} = g\beta\eta [J_{|\nu-\alpha|}(\omega t)]^2 \quad (58)$$

under the conditions (41), (51), and the one in and below Eq. (57). For small t this implies the same approximation as in Eq. (55), while for large t one now obtains

$$\langle s_\alpha^z \rangle_t - \langle s_\alpha^z \rangle_{\text{th}} = \frac{2g\beta\eta}{\pi} \frac{\cos^2(\omega t \pm \pi/4)}{\omega t}, \quad (59)$$

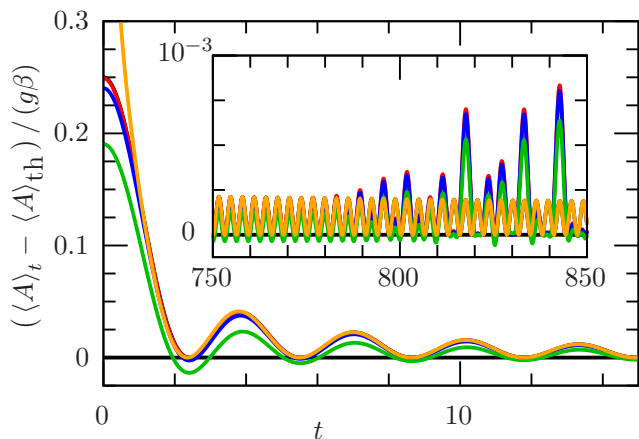


FIG. 6. Numerical evaluation of Eq. (17) divided by $g\beta$ for $L = 800$ and $\beta = 0.2$ (red), $\beta = 0.6$ (blue), $\beta = 2$ (green). The orange curve depicts the large- t asymptotics from Eq. (59). The approximation (58) would be indistinguishable from the red curve in the main plot and from the orange curve in the inset, and is therefore not shown. Everything else as in Fig. 1.

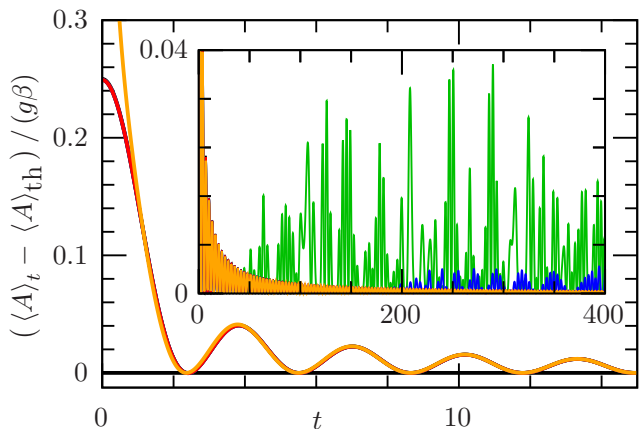


FIG. 7. Same as in Fig. 6 but for $\beta = 0.2$ and $L = 800$ (red), $L = 200$ (blue), $L = 50$ (green). Up to $t \approx 50$, the green curves are covered by the red curves, and likewise for the blue curves up to $t \approx 200$. In turn, the orange curves almost cover the red curves between $t \approx 1$ and $t \approx 800$. Beyond $t \approx 800$, the deviations between the red and orange curves would still be hardly discernible on the scale of the present inset, hence we actually plotted only t -values up to 400.

where, as in Eq. (56), the plus sign applies if $\nu - \alpha$ is odd, and the minus sign otherwise. Furthermore, analogous remarks as below Eq. (56) and in the paragraph below Eq. (54) apply. In particular, $\omega t \gg |(\nu - \alpha)^2 - 1/4|$ (see below Eq. (F8)) is known to be yet another sufficient (but possibly not necessary) prerequisite for the approximation of Eq. (58) by Eq. (59).

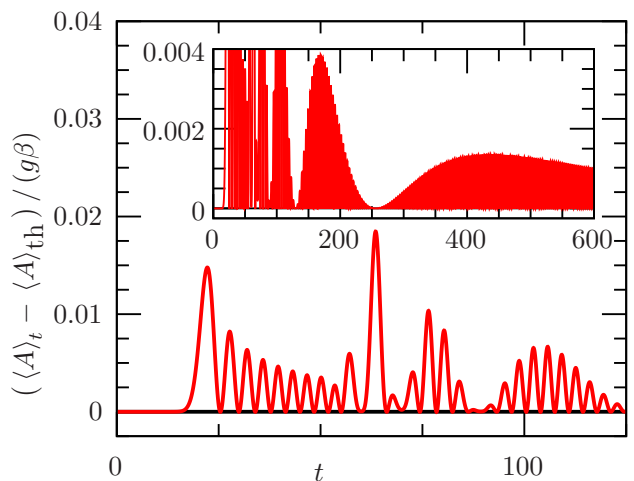


FIG. 8. Numerical evaluation of Eq. (17) divided by $g\beta$ for $\nu = 20$, $\alpha = 40$, $L = 800$, and $\beta = 0.2$. The approximation from Eq. (53) is indistinguishable from the red curve on the scale of this plot. Everything else as in Fig. 1.

1. Discussion

The prediction (58) is mainly based on the three assumptions (41), (51), and (57). In practice, the condition (41) essentially amounts to a small- β (large temperature) approximation. The main plot in Fig. 6 quantitatively illustrates this predicted convergence of Eq. (17) towards Eq. (58) upon decreasing β . Furthermore, the approximation (59) is depicted in orange. Similarly, the main plot in Fig. 7 is meant to illustrate the condition (57), demonstrating the convergence of Eq. (17) towards Eq. (58) upon increasing L . The breakdown of the approximation (59) below $t \approx 1$ (orange curves in Figs. 6 and 7) can be understood via the prerequisite mentioned below Eq. (59). On the other hand, the insets in Figs. 6 and 7 numerically demonstrate that also the restriction to moderately large t as quantified by Eq. (51) is indeed necessary for the validity of the approximations (58) and (59). For the rest, the findings in those insets are again closely related to the discussion in the third paragraph of Sec. IV A 1.

An analogous comparison of Eq. (17) with the approximation (53) is exemplified by Fig. 8. The main difference compared to all previous numerical examples is the choice of $\nu = 20$ and $\alpha = 40$, i.e., the perturbation and the observable are neither close to each other, nor close to the chain-end, nor really deep in the “bulk” of the chain. The first main message of Fig. 8 is that the approximation (53) agrees with Eq. (17) very well at least for the depicted times $t \in [0, 600]$. On the other hand, the approximation (56) is found to strongly disagree from the curves in Fig. 8 and is therefore not plotted. Indeed, according to the extra prerequisite mentioned below Eq. (56), a reasonably good agreement is only expected for much larger t values than those shown in Fig. 8. On the other

hand, the good agreement of Eq. (17) with Eq. (53) (and possibly with Eq. (56)) is expected to break down when Eq. (51) is violated, i.e., beyond $t \approx L$. Since all this is similar as in Figs. 6 and 7, we did not show it once again in Fig. 8.

Much more interesting appears to us to gain a better understanding of the quite intricate findings for $t \in [0, 600]$ in Fig. 8. This is possible with the help of the following result from Appendix F:

For moderate-to-large values of k , the Bessel functions $J_k(t)$ are negligibly small for all $t < ck$ with some k -independent constant c , which is numerically found to be close to unity (and can be analytically lower bounded by 0.38, see Appendix F). Similarly as at the end of Sec. IV A 1, this may be viewed as a consequence and quantitative illustration of some suitable Lieb-Robinson bounds [30–34], where $1/c \approx 1$ plays the role of a speed at which the information that there has been a quantum quench at time $t = 0$ travels through the chain. Accordingly, both Bessel functions in Eq. (53) are negligible (practically no signal is observable) up to times of the order of the distance $|\nu - \alpha|$ between perturbation and observable. Subsequently, the first Bessel function in Eq. (53) is no longer negligible, while the second still remains negligible up to times of the order $\nu + \alpha$. The latter can be interpreted as the signal’s traveling time from the perturbation site ν to the left chain end, plus the traveling time of the reflected signal to the measurement site α .

At even later times, both Bessel functions in Eq. (53) notably contribute and ultimately result in the asymptotics (56). However, before this asymptotics actually sets in, quite complicated “interference effects” of the two Bessel functions in Eq. (53) are expected and indeed observed in Fig. 8.

The only relevant remaining case is when $|\nu - \alpha|$ is large (implying that also $\nu + \alpha$ and $2L - (\nu + \alpha)$ must be large). Similarly as above Eq. (58) we thus may consider both summands on the right-hand side of Eq. (46) as negligible, in agreement with what one intuitively would have expected: A local perturbation does not notably affect sufficiently remote observables.

From the well-known properties of $J_k(t)$ collected in Appendix F it seems reasonable to expect that $J_k(t) \rightarrow 0$ for $k \rightarrow \infty$ uniformly in t (though we were not able to rigorously prove it). If so, we see that (53) already includes (58) as a special case. In fact, (53) will even remain valid for arbitrary ν and α , except in situations where both ν and α are close to L . (The behavior in the latter situations can be readily recovered by the symmetry argument in the paragraph below Eq. (56).) The only remaining validity conditions for Eq. (53) are then Eq. (51) and $L \gg 1$. However, the different asymptotic results in Eqs. (56) and (59) indicate that things are actually more subtle, at least as far as the sequence of the limits $\nu + \alpha \rightarrow \infty$ and $t \rightarrow \infty$ are concerned [35]. Further such caveats are: (i) The dependence on $|\nu - \alpha|$ in Eq. (58) has apparently completely disappeared from the

large-time asymptotics (59). However, this dependence still appears via the pertinent validity condition mentioned below Eq. (59). (ii) The asymptotics (56) should go over into Eq. (59) upon increasing ν and α (provided Eq. (57) stays satisfied). However, in doing so the factors $\nu^2 \alpha^2$ in Eq. (56) increase quite strongly. On the other hand, Eq. (56) decreases as t^{-3} and Eq. (59) only as t^{-1} . Closer inspection shows that the validity conditions below Eqs. (56) and (59) are such that the factors $\nu^2 \alpha^2$ may indeed “compensate” the different powers of t in just the right way to be still compatible with a smooth transition between the two asymptotic results.

D. Generalization

Throughout the previous Subsection IV C we assumed that the condition (41) is fulfilled. Here, we briefly outline how one may proceed without this assumption.

The key idea is to consider instead of the original quantity in Eq. (17) its (negative) derivative

$$v(t) := -\frac{d}{dt}(\langle s_\alpha^z \rangle_t - \langle s_\alpha^z \rangle_{\text{th}}). \quad (60)$$

Together with Eqs. (19), (20), and (44) we thus can conclude (after a short calculation) that

$$v(t) = g \operatorname{Im}(W(t)B^*(t)), \quad (61)$$

$$B(t) := \sum_{n=1}^L \tilde{S}_n^\nu \tilde{S}_n^\alpha \tanh(\beta \tilde{E}_n / 2) e^{-i\tilde{E}_n t}. \quad (62)$$

Finally, we can integrate $v(t)$ from Eq. (60), yielding

$$\langle s_\alpha^z \rangle_t - \langle s_\alpha^z \rangle_{\text{th}} = \langle s_\alpha^z \rangle_{t'} - \langle s_\alpha^z \rangle_{\text{th}} + \int_t^{t'} d\tau v(\tau). \quad (63)$$

According to the thermalization property from Sec. IV A, the expectation values $\langle s_\alpha^z \rangle_{t'}$ must stay very close to $\langle s_\alpha^z \rangle_{\text{th}}$ for the vast majority of all sufficiently late times t' provided the system size L is sufficiently large. Hence the first two terms on the right-hand side of Eq. (63) can be considered to approximately cancel each other, symbolically indicated as

$$\langle s_\alpha^z \rangle_t - \langle s_\alpha^z \rangle_{\text{th}} = \int_t^\infty d\tau v(\tau). \quad (64)$$

For large L , the function $W(t)$ in Eq. (61) can again be approximated by Eqs. (46) and (49) or (50). Likewise, the function $B(t)$ in Eq. (62) can be rewritten as

$$B(t) = e^{i|G|t} \left[\tilde{B}_{|\nu-\alpha|}(\omega t) - \tilde{B}_{\nu+\alpha}(\omega t) \right], \quad (65)$$

where $\tilde{B}_k(t)$ can be approximated for large L as

$$\tilde{B}_k(t) = \frac{1}{\pi} \int_0^\pi dx \cos(kx) T_\beta(x) \exp\{it \cos(x)\}, \quad (66)$$

$$T_\beta(x) := -\tanh(\beta[|J| \cos(x) + |G|]/2). \quad (67)$$

A central point of our present approach is that all three approximations in Eqs. (49), (64), and (66) become asymptotically exact as $L \rightarrow \infty$.

In the absence of $T_\beta(x)$ in Eq. (66), the functions $\tilde{B}_k(t)$ would be identical to $\tilde{W}_k(t)$ from Eq. (49), and could be related to the Bessel functions $J_k(t)$ as in Eq. (50). In the presence of $T_\beta(x)$ in Eq. (66), an analogous relation to some well-established special functions does not seem to exist. Put differently, we could consider Eq. (66) as the definition of a new special function and then determine its basic properties analogously to the basic properties of the Bessel functions in Appendix F. However, this goes beyond the scope of our present paper, with the exception of one particularly simple example, to which we now turn.

As in Eqs. (56) and (59) we focus on large times. Moreover, we take for granted the condition (51), the conditions in and below Eq. (57) together with

$$\alpha = \nu \quad (68)$$

(perturbation and observable identical and far from the chain ends), and the condition

$$G = 0 \quad (69)$$

(no transversal field in Eq. (7)). Similarly as below Eq. (57), we thus can neglect the last term in Eq. (46) and likewise for the last term in Eq. (65). Utilizing Eqs. (50), (61), and the fact that the $J_k(t)$ are real functions of t this yields

$$v(t) = -g J_0(\omega t) \text{Im}(\tilde{B}_0(\omega t)) . \quad (70)$$

As detailed in Appendix G, the explicit evaluation of the right-hand side under the above specified conditions is possible but somewhat tedious, resulting in the approximation

$$v(t) = \frac{2g}{\pi} \left(-\frac{b_0 c(t) s(t)}{\omega t} + \frac{b_1 c^2(t) - \frac{b_0}{8} s^2(t)}{(\omega t)^2} \right) , \quad (71)$$

$$c(t) := \cos(\omega t - \pi/4), \quad s(t) := \sin(\omega t - \pi/4), \quad (72)$$

$$b_0 := -\tanh(\beta|J|/2), \quad b_1 = \frac{b_0}{8} + \frac{\beta|J|}{4 \cosh^2(\beta J/2)}, \quad (73)$$

where corrections of the order of $(\omega t)^{-5/2}$ have been omitted on the right-hand side of Eq. (71). Hence, the integral in Eq. (64) can be evaluated, yielding

$$\langle s_\alpha^z \rangle_t - \langle s_\alpha^z \rangle_{\text{th}} = \frac{g}{\pi J} \frac{\tanh(\frac{\beta J}{2}) c^2(t) - r(\frac{\beta J}{2})}{\omega t} \quad (74)$$

apart from higher order corrections in $1/\omega t$, and where

$$r(x) := \frac{\tanh(x)}{2} - \frac{x}{2 \cosh^2(x)} . \quad (75)$$

One readily confirms that $r(x)$ is an odd and monotonically increasing function of x , scaling as x^3 for small x , and approaching $1/2$ for large x . We also note that $|J|$

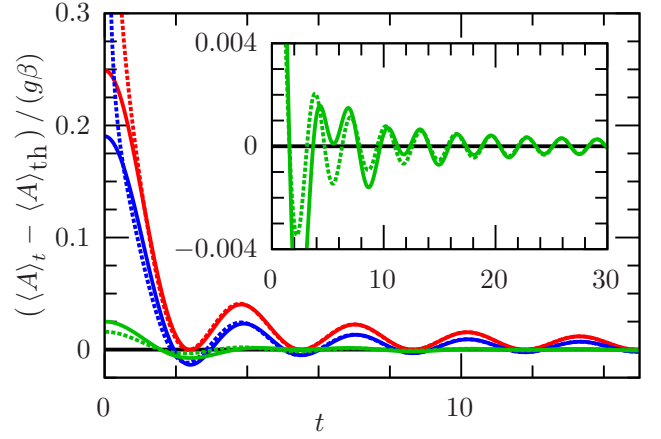


FIG. 9. Solid: Numerical evaluation of Eq. (17) divided by $g\beta$ for $L = 800$ and $\beta = 0.2$ (red), $\beta = 2$ (blue), $\beta = 20$ (green). Everything else as in Fig. 1. Dotted: The corresponding large- t asymptotics from Eq. (74).

has been replaced by J in Eq. (74) since the right-hand side is invariant under such a replacement. Fig. 9 illustrates the quality of the large- t asymptotics (74).

In particular, for high temperatures (i.e. $|\beta J| \ll 1$, see also Eqs. (6) and (41)) one recovers Eq. (59) from Eq. (74) (under the extra conditions (68) and (69)). Turning to low temperatures, one can deduce from Eqs. (74) and (75) that

$$\langle s_\alpha^z \rangle_t - \langle s_\alpha^z \rangle_{\text{th}} = \frac{g}{\pi J} \frac{\sin(2\omega t)}{\omega t} \quad \text{for } \beta J \gg 1, \quad (76)$$

and analogously for $\beta J \ll -1$.

More generally, the main difference between the high-temperature approximation (43) (see also Eqs. (53)-(59)) and the results (74), (76) for general temperatures is that the former is strictly non-negative, while the latter exhibits sign changes, see also Fig. 9.

V. FURTHER EXAMPLES

Generalizing Eq. (16), we now turn to perturbations V and observables A of the form

$$V = s_\nu^a, \quad A = s_\alpha^b \quad (77)$$

with $a, b \in \{x, y, z\}$.

The case $a = b = z$ has been treated in Sec. IV. In the case $a = z$ and $b \neq z$ one readily can infer from Eqs. (14), (B43), and (B44) the trivial result $\langle A \rangle_t = \langle A \rangle_{\text{th}} = 0$ independent of t . In other words, the perturbation does not drive the observable out of equilibrium. Similarly, one finds for $b = z$ and $a \neq z$ that $\langle A \rangle_t = \langle A \rangle_{\text{th}}$. For a more detailed discussion of the latter expectation value $\langle A \rangle_{\text{th}} = \langle s_\alpha^z \rangle_{\text{th}}$ we refer to Appendix E.

Altogether we thus can conclude that for any given perturbation V of the form s_ν^z the system exhibits thermalization at least as far as all single-site observables A

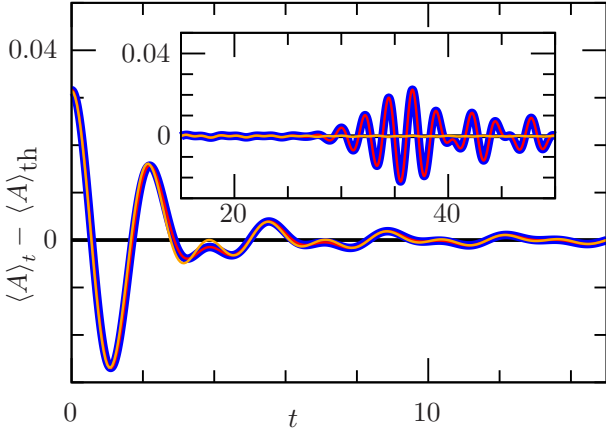


FIG. 10. Blue: Numerically exact results for the same system as in Fig. 1 (a) but now for $A = V = s_1^x$ and $G = 2\sqrt{2}$. Red: Analytical approximation from Eq. (78). Orange: Approximation (83). Main plot: Initial relaxation behavior. Inset: Transition from moderate- to long-time behavior.

of the form Eq. (77) are concerned (see also Sec. II). The same applies to perturbations of the form $V = s_\nu^{x,y}$ in combination with observables of the form $A = s_\alpha^z$.

The remaining cases are (i) $a = b = x$ and (ii) $a = y$, $b = x$. [The two other cases $a = b = y$ and $a = x$, $b = y$ then readily follow by symmetry arguments.] In the special case $\nu = \alpha = 1$ one obtains, similarly as in Eq. (17), by means of the methods from Appendix C the result

$$\langle s_1^x \rangle_t - \langle s_1^x \rangle_{\text{th}} = \frac{g\beta}{2} \text{Re}(X(t)) \quad \text{if } V = s_1^x, \quad (78)$$

$$\langle s_1^x \rangle_t - \langle s_1^x \rangle_{\text{th}} = \frac{g\beta}{2} \text{Im}(X(t)) \quad \text{if } V = s_1^y, \quad (79)$$

$$X(t) := \sum_{n=1}^L (\tilde{S}_n^1)^2 \frac{\tanh(\beta \tilde{E}_n/2)}{\beta \tilde{E}_n} e^{-i\tilde{E}_n t}. \quad (80)$$

In the same way as below Eq. (24), one can conclude that Eq. (78) must be an odd function of β , and an even function of J and of G , while Eq. (79) must be an even function of J , and an odd function of β and of G . Fig. 10 exemplifies the very good agreement between the analytical approximation from Eq. (78) (red) and numerically exact results (blue).

Similarly as in Sec. IV A one can show that the long-time average $\overline{X(t)}$ is a real number between zero and $1/L$, and that $|\overline{X(t)}|^2 = \overline{\text{Re}(X^2(t))} + \overline{\text{Im}(X^2(t))}$ is upper bounded by $1/2L$, implying that the observables in Eqs. (78) and (79) exhibit thermalization.

Similarly as in Sec. IV C, taking for granted that Eq. (41) is fulfilled we may employ the approximation

$$\frac{\tanh(\beta \tilde{E}_n/2)}{\beta \tilde{E}_n} \simeq \frac{\tanh(\beta G/2)}{\beta G} =: \kappa. \quad (81)$$

As in Eqs. (43)-(48) it then follows that

$$X(t) = \kappa e^{iGt} [\tilde{W}_0(\omega t) - \tilde{W}_2(\omega t)] \quad (82)$$

and that the functions $\tilde{W}_k(t)$ may be approximated by Bessel functions of the first kind according to Eq. (50). Note that, unlike in Eq. (46), the quantity G must appear in Eq. (82) without the absolute sign to properly reproduce the symmetry properties below Eq. (80), see also Eq. (47). Under the conditions (51) and (52) we thus obtain, similarly as in Eq. (53), the approximation

$$\langle s_1^x \rangle_t - \langle s_1^x \rangle_{\text{th}} = \frac{g\beta\kappa}{2} L(t) [J_0(\omega t) + J_2(\omega t)], \quad (83)$$

where

$$L(t) := \begin{cases} \cos(Gt) & \text{if } V = s_1^x \\ \sin(Gt) & \text{if } V = s_1^y \end{cases} \quad (84)$$

In the same way as in Eq. (56), this implies the large- t asymptotics

$$\langle s_1^x \rangle_t - \langle s_1^x \rangle_{\text{th}} = \sqrt{\frac{2}{\pi}} g\beta\kappa L(t) \frac{\sin(\omega t - \pi/2)}{(\omega t)^{3/2}}. \quad (85)$$

The approximation (83) is illustrated by the orange curve in Fig. 10. In accordance with the pertinent preconditions (41), (51), (52), the agreement with the numerically exact behavior (blue) is seen to be very good up to times t of the order of L . [More precisely, the threshold is near $t = 2L = 32$.] For even larger times, the situation is analogous to the discussion at the end of Sec. IV A 1 and at the beginning of Sec. IV C 1. Similarly as in Fig. 6, the approximation (85) would be indistinguishable from Eq. (83) beyond $t = 1$ in Fig. 10 and is therefore not shown. The specific choice of G in Fig. 10 results in oscillations of $L(t)$ in Eq. (85) with frequency $G = 2\sqrt{2}$ according to Eq. (84), while the last term in Eq. (85) oscillates with frequency $\omega = 1$. The resulting interference of the two oscillations explains the quite non-trivial time-dependence in the main plot of Fig. 10.

Analogous results apply for the observable $A = s_1^y$ instead of $A = s_1^x$, and for the chain sites $\nu = \alpha = L$ instead of $\nu = \alpha = 1$. All the remaining cases are well-known to be technically more demanding due to the non-locality issues of the Jordan-Wigner transformation pointed out at the end of Appendix A 1. Accordingly, explicit analytical results for the correlations in Eqs. (13) and (14) are only available in the literature for asymptotically large or small values of β , see for instance in Refs. [31, 39–41] and further references therein. Most notably, for $L \rightarrow \infty$, sufficiently small β , perturbations of the form $V = s_\nu^x$, and under the conditions in and around Eq. (57) one finds the asymptotic approximation

$$\langle s_\alpha^x \rangle_t - \langle s_\alpha^x \rangle_{\text{th}} = \delta_{\nu\alpha} \frac{g\beta}{4} \cos(Gt) e^{-\omega^2 t^2/4}. \quad (86)$$

Moreover, for sufficiently large times this superexponential decay is known to ultimately cross over into an ordinary exponential decay whenever $\beta \neq 0$ [31, 35].

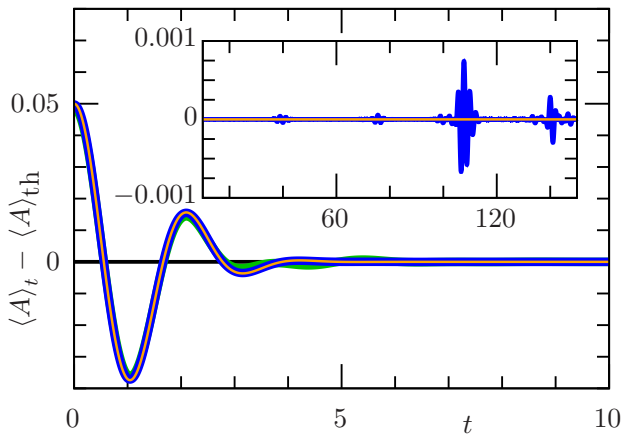


FIG. 11. Blue: Numerically exact results for the same system as in Fig. 1 (a) but now for $A = V = s_{L/2}^x$, $G = 2\sqrt{2}$, $g = 4$, and $\beta = 0.05$. Green: same but for $g = 1$ and $\beta = 0.2$. Orange: Large- L and small- β asymptotics from Eq. (86). Main plot: Initial relaxation behavior. Inset: Transition from moderate- to long-time behavior (the green curve is omitted).

A comparison of the approximation (86) with numerically exact results is provided in Fig. 11. Similarly as in Fig. 10, the agreement is very good up to times t of the order of L , but not any more for substantially larger times (inset), while the details of the latter disagreement are quite different in the two figures. Note that a theoretical prediction corresponding to the red curve in Fig. 10 is not available in the case of Fig. 11. Moreover, the approximation (86) requires β to be even smaller than the corresponding approximation (83) in Fig. 10, as can be inferred upon comparison of the green and blue curves in Fig. 11.

Since analytical results for finite L are not available in our present case, we cannot verify thermalization in the same way as in our previous examples. However, if one takes for granted that the limits $L \rightarrow \infty$ and $t \rightarrow \infty$ can be exchanged (as it is often done), and that the derivation of the above-mentioned results can be considered as sufficiently rigorous, thermalization follows immediately from those results.

We recall that Eq. (86) applies if $V = s_\nu^x$. Upon comparison with Eq. (83) it is natural to conjecture that a sine instead of the cosine will appear on the right-hand side of Eq. (86) if $V = s_\nu^y$. Appendix I provides a more careful justification of this conjecture (see Eq. (I1) therein).

A. Synopsis and extensions

Let us finally collect the various findings of this and the previous sections. As stated below Eq. (77), we covered all single-site observables $A = s_\alpha^b$ for arbitrary perturbations of the form $V = s_\nu^z$. In particular, thermaliza-

tion and various more detailed properties of the time-dependent expectation values have been deduced under the proviso that the parameter ϵ in Eq. (15) remains sufficiently small. With respect to the remaining cases mentioned above Eq. (78), we also covered many particularly interesting single-site observables for perturbations of the form $V = s_\nu^{x,y}$. An analogous treatment of the remaining single-site observables is expected to be in principle straightforward, but in practice the required calculations are, as explained above Eq. (86), well known to be a very daunting task, which goes beyond the scope of our present work. Essentially the same applies to observables A or perturbations V which consist of a product of several single-spin operators.

Further modifications and extensions, which are expected to be technically less challenging but nevertheless omitted here, include XX-models with periodic instead of the open boundary conditions in Eq. (7), and so-called XY-models with different couplings of the nearest neighbor interactions of the x - and y -spins in Eq. (7), see also Refs [22, 42].

Finally, yet another kind of generalization is obvious, yet noteworthy. Given some perturbation V with its above specified class of “admitted” observables A , arbitrary linear combinations of those observables will obviously be admitted as well. Formally, the reason is that Eq. (3) is linear in A . Moreover, also the quantitative properties (including thermalization) immediately follow by linearity from the known properties of the summands. Likewise, given some observable A with its concomitant class of “admitted” perturbations V , linear combinations of those perturbations are again admissible due to the fact that the right-hand side of Eq. (14) is linear in V . Moreover, the quantitative behavior of the given observable A again follows by linearity. However, an additional requirement is now that the parameter ϵ in Eq. (15) must still be small for the perturbation V under consideration. In particular, extensive perturbations (corresponding to a global quench scenario) are thus excluded in the thermodynamic limit $L \rightarrow \infty$, as already mentioned below Eq. (15) and in Sec. IV B.

VI. CONCLUSIONS

This section complements the general considerations in Secs. I and II, which are therefore not repeated here.

The two main achievements of our present work are a rigorous demonstration of thermalization and a detailed analytical as well as numerical exploration of the temporal relaxation behavior. For this purpose we focused on a particularly simple model, namely the XX-spin chain from Eq. (7), on particularly simple initial states, essentially amounting to weak local quantum quenches, and on single-site observables and sums thereof, as detailed in the previous Sec. V A. On the one hand, one may say that these assumptions and restrictions are rather strong. On the other hand, in view of how little is rigorously known

with regard to thermalization (see also Sec. II), it seems unavoidable to get used to some degree of modesty in this context.

Despite the simplicity of the model, its detailed temporal behavior turned out to be very rich, ranging from damped oscillations with a possibly very slow algebraic decay, to complicated interferences of several such damped oscillations, to a superexponential (Gaussian) decay in time. The latter is ultimately caused by the non-local character of the pertinent Jordan-Wigner transformation and shows that our present simple example already goes beyond the realm of “effectively” non-interacting theories in combination with local observables, see e.g. Refs. [43, 44] and numerous further references cited therein. Moreover, those non-interacting theories are also complementary to our present work in that they cover a considerably more general class of (integrable) models and initial conditions, while no analytical results with respect to the issue of thermalization are obtained (instead, so-called generalized Gibbs ensembles often play a central role).

A specific virtue of our present approach is that one can explore in quite some detail the system’s behavior for a possibly very large but fixed time-point t when the chain-length L becomes arbitrarily large (thermodynamic limit), but also for a possibly very large but finite L when t becomes arbitrarily large. Most importantly, the behavior in one case turned out to hardly admit any conclusions regarding the other case (see Secs. IV A 1, IV C 1, and V). Therefore, the relevance of analytical results in the thermodynamic limit with respect to the long-time behavior of real (finite) systems may be less obvious than what is often suggested in the literature.

We furthermore remark that there exists a considerable variety of related but different analytical investigations, dealing with entire statistical ensembles of models [45], and resulting in predictions which apply with very high probability to a *randomly sampled* member of the ensemble. However, and in contrast to our present approach, with respect to a *given* (non-random) model system, there always remains some uncertainty. Even more serious issues are: (i) The same, given model may possibly be viewed as a member of two different ensembles, each of which predicts a different behavior with high probability. (ii) In order to be analytically tractable, certain basic properties of the given model are often no longer true for the vast majority of all the other members of the ensemble. For instance, the system of actual interest may exhibit only short-range and few-body interactions (such as our present model from Eq. (7)), but *not* the vast majority of the other members of the ensemble.

In our present study we mainly focused on quenches and observables each of which acts nontrivially on only one site of the spin chain (and on sums of such observables). Various generalizations are in principle straightforward, while the technical details (for instance in Appendix B 1) will often be substantially more involved, see also Sec. V A.

Further extensions which may be worthwhile to be explored in the future include generalizations beyond the realm of weak local perturbations and of our simple XX-spin-chain model (7). Specifically, we are aware of a variety of non-rigorous arguments according to which thermalization after a *local* quench might appear as being almost trivial even for much more general models than in Eq. (7). However, such arguments may be misleading in view of the following result, which will be elaborated in a separate work. Namely, *absence* of thermalization after a local quench can be analytically shown to occur for a slight modification of our present setup in Eqs. (7)-(9). In other words, minor details may be of great importance regarding the issue of thermalization, and rigorous results are therefore quite valuable even for apparently very simple models.

ACKNOWLEDGMENTS

We thank Jannis Eckseler for valuable numerical assistance. This work was supported by the Deutsche Forschungsgemeinschaft (DFG, German Research Foundation) under Grant No. 355031190 within the Research Unit FOR 2692 and under Grant No. 502254252, and by the Paderborn Center for Parallel Computing (PC²) within the project HPC-PRF-UBI2.

Appendix A: Jordan-Wigner Transformation and beyond

This Appendix summarizes the main steps of the so-called Jordan-Wigner transformation, and discusses some implications of specific interest in our present paper. Since this transformation is well-established basic knowledge, we only mention here once and for all a very incomplete selection of pertinent previous works, see Refs. [22, 31, 39–42] and further references therein. On the other hand, we will include sufficient details to make the calculations self-contained. Since such calculations may also be of interest in other contexts, we actually consider somewhat more general model Hamiltonians than in Eq. (7) of the main paper, namely

$$H = - \sum_{l=1}^{L-1} J_l (s_{l+1}^x s_l^x + s_{l+1}^y s_l^y) - \sum_{l=1}^L G_l s_l^z. \quad (\text{A1})$$

Similarly as below Eq. (7), it is well-known (and can be readily verified by means of the subsequent formalism) that $S^z := \sum_{l=1}^L s_l^z$ is still a conserved quantity, i.e., $[H, S^z] = 0$, for arbitrary J_l and G_l .

1. Standard Jordan-Wigner Transformation

As usual (see also below Eq. (7)), it is convenient to employ the eigenbasis of the spin operators s_l^z , implying that $s_l^a = \sigma_l^a/2$, where the σ_l^a are Pauli-matrices and $a \in \{x, y, z\}$. Moreover, all operators are understood as acting on the system's full many-body Hilbert space (tensor product of L spin-1/2 spaces), hence Pauli matrices with different indices l always commute with each other.

Defining the usual raising and lowering operators as $\sigma_l^\pm := (\sigma_l^x \pm i\sigma_l^y)/2$ and exploiting that the σ_l^a are Pauli matrices one readily verifies that

$$\sigma_l^x = \sigma_l^+ + \sigma_l^-, \quad (\text{A2})$$

$$\sigma_l^y = (\sigma_l^+ - \sigma_l^-)/i, \quad (\text{A3})$$

$$\sigma_l^z = 2\sigma_l^+ \sigma_l^- - 1, \quad (\text{A4})$$

$$\sigma_l^z \sigma_l^\pm = \pm \sigma_l^\pm. \quad (\text{A5})$$

Hence, the Hamiltonian (A1) can be rewritten as

$$H = \tilde{H} + G_{tot} \quad (\text{A6})$$

with

$$\tilde{H} := -\frac{1}{2} \sum_{l=1}^{L-1} J_l (\sigma_{l+1}^+ \sigma_l^- + \sigma_l^+ \sigma_{l+1}^-) - \sum_{l=1}^L G_l \sigma_l^+ \sigma_l^- \quad (\text{A7})$$

and

$$G_{tot} := \frac{1}{2} \sum_{l=1}^L G_l. \quad (\text{A8})$$

Next we define the so-called string operators

$$Z_l := \prod_{k=1}^{l-1} (-\sigma_k^z) \quad (\text{A9})$$

and the creation and annihilation operators

$$c_l^\dagger := \sigma_l^+ Z_l, \quad (\text{A10})$$

$$c_l := (c_l^\dagger)^\dagger = Z_l \sigma_l^-. \quad (\text{A11})$$

Some useful technical side remarks are: (i) $Z_1 = 1$, implying $c_1^\dagger = \sigma_1^+$ and $c_1 = \sigma_1^-$. (ii) Z_l commutes with σ_l^\pm , implying $c_l^\dagger = Z_l \sigma_l^+$ and $c_l = \sigma_l^- Z_l$. (iii) Since $(\sigma_l^z)^2 = 1$ we find $Z_l^2 = 1$, implying $\sigma_l^+ = Z_l c_l^\dagger = c_l^\dagger Z_l$, $\sigma_l^- = Z_l c_l = c_l Z_l$, and $\sigma_l^+ \sigma_l^- = c_l^\dagger c_l$. (iv) Exploiting Eq. (A5) it follows that $\sigma_{l+1}^+ \sigma_l^- = c_{l+1}^\dagger c_l$.

We thus can rewrite Eqs. (A2)-(A4), (A7), and (A9) as

$$\sigma_l^x = Z_l (c_l^\dagger + c_l), \quad (\text{A12})$$

$$\sigma_l^y = Z_l (c_l^\dagger - c_l)/i, \quad (\text{A13})$$

$$\sigma_l^z = 2c_l^\dagger c_l - 1, \quad (\text{A14})$$

$$\tilde{H} = -\frac{1}{2} \sum_{l=1}^{L-1} J_l (c_{l+1}^\dagger c_l + c_l^\dagger c_{l+1}) - \sum_{l=1}^L G_l c_l^\dagger c_l, \quad (\text{A15})$$

$$Z_l = \prod_{k=1}^{l-1} (1 - 2c_k^\dagger c_k). \quad (\text{A16})$$

Similarly as in Eqs. (A2)-(A5) one readily verifies that

$$\{\sigma_l^+, \sigma_l^-\} = 1, \quad (\text{A17})$$

$$\{\sigma_l^+, \sigma_l^+\} = \{\sigma_l^-, \sigma_l^-\} = 0, \quad (\text{A18})$$

where $\{A, B\} := AB + BA$ (anti-commutator). Furthermore, by combining Eq. (A5) with its adjoint counterpart $\sigma_l^\mp \sigma_l^z = \pm \sigma_l^\mp$ one sees that

$$\sigma_l^z \sigma_l^\pm = -\sigma_l^\pm \sigma_l^z, \quad (\text{A19})$$

and with Eq. (A9) that

$$Z_k \sigma_l^\pm = \begin{cases} \sigma_l^\pm Z_k & \text{if } k \leq l \\ -\sigma_l^\pm Z_k & \text{if } k > l \end{cases} \quad (\text{A20})$$

Together with Eqs. (A10), (A11), (A17), (A18) we thus can infer the anti-commutation relations

$$\{c_k^\dagger, c_l\} = \delta_{kl}, \quad \{c_k, c_l\} = \{c_k^\dagger, c_l^\dagger\} = 0 \quad (\text{A21})$$

for all $k, l \in \{1, \dots, L\}$, where δ_{kl} is the Kronecker delta. In other words, the c_l^\dagger and c_l are indeed fermionic creation and annihilation operators.

We remark that the operators σ_l^\pm fulfill analogous anti-commutation relations as in Eq. (A21) if $k = l$ (see Eqs. (A17) and (A18)), but in general not any more if $k \neq l$. (Instead, they fulfill the commutation relations $[\sigma_k^+, \sigma_l^-] = \delta_{kl} \sigma_k^z$, $[\sigma_k^+, \sigma_l^+] = 0$, and $[\sigma_k^-, \sigma_l^-] = 0$.) This is the main advantage of the above Jordan-Wigner transformation from the operators σ_l^+ and σ_l^- to the operators c_l^\dagger and c_l . A notable disadvantage is that Eqs. (A9)-(A11) are, in general, non-local operators (with respect to the actual model of interest in Eq. (A1)). Analogously, the basic observables Eqs. (A12) and (A13) of the original model are generally non-local operators of the transformed model (see also Eq. (A16)).

More precisely speaking, since $Z_1 = 1$ (see below Eq. (A11)) the transformed observables Eqs. (A12) and (A13) remain local for $l = 1$, and similarly for a few more (small) l -values (near the left chain end). Likewise, by replacing $\prod_{k=1}^{l-1}$ on the right-hand side of Eq. (A9) by $\prod_{k=l+1}^L$, the transformed observables would remain local near the right chain end (more physically, this essentially amounts to interchanging the chain ends). However, away from both chain ends, the non-locality remains a non-trivial issue, see also the discussion above Eq. (86) in the main paper.

2. Diagonalization

Instead of the specific Hamiltonians from Eq. (A15) let us temporarily consider a general ‘‘quadratic’’ Hamiltonian of the form

$$\tilde{H} = \sum_{k,l=1}^L B_{kl} c_k^\dagger c_l, \quad (\text{A22})$$

with arbitrary coefficients B_{kl} apart from the hermiticity condition $B_{lk} = B_{kl}^*$. Considering the B_{kl} as the matrix elements of a Hermitian $L \times L$ matrix B , it follows that there exists a unitary matrix U with the property $U^\dagger D U = B$, where D is a diagonal Hermitian matrix. In other words its matrix elements are of the form $D_{kl} = \delta_{kl} \tilde{E}_k$ with real diagonal elements \tilde{E}_k . Denoting by c a column vector (or vector-operator) with entries (elements) c_l , and by c^\dagger the concomitant row vector with entries c_l^\dagger , we can rewrite Eq. (A22) as $\tilde{H} = c^\dagger B c = f^\dagger D f$, where $f := U c$ is a column vector with entries

$$f_k := \sum_{l=1}^L U_{kl} c_l, \quad (\text{A23})$$

and f^\dagger the concomitant row vector with entries $f_k^\dagger = (f_k)^\dagger$. In other words, Eq. (A22) takes the form

$$\tilde{H} = \sum_{k=1}^L \tilde{E}_k f_k^\dagger f_k. \quad (\text{A24})$$

Exploiting Eqs. (A21) and (A23) we can conclude that

$$\{f_k^\dagger, f_l\} = \delta_{kl}, \quad \{f_k, f_l\} = \{f_k^\dagger, f_l^\dagger\} = 0, \quad (\text{A25})$$

i.e., the f_l^\dagger and f_l are again fermionic creation and annihilation operators.

Let us denote by $|0\rangle := |\downarrow \cdots \downarrow\rangle$ the specific L -spin product state where every single spin is in the “down” state in the eigenbasis of s_l^z , i.e., $\sigma_l^z |0\rangle = -|0\rangle$ for all l . Exploiting that $\sigma_l^- := (\sigma_l^x - i\sigma_l^y)/2$ (see above Eq. (A2)) one can infer that $\sigma_l^- |0\rangle = 0$ for any $l \in \{1, \dots, L\}$, implying with Eq. (A11) that $c_l |0\rangle = 0$ and with Eq. (A23) that

$$f_l |0\rangle = 0 \quad (\text{A26})$$

for any $l \in \{1, \dots, L\}$. Alternatively, $|0\rangle$ may thus be viewed as “vacuum state”, especially with reference to fermionic Hubbard-like models as in Eq. (A15).

Next we denote by $\vec{b} := (b_1, \dots, b_L)$ a vector with L “binary” components $b_k \in \{0, 1\}$, i.e., there are 2^L different such vectors. For any given \vec{b} , we furthermore define the state

$$|\vec{b}\rangle := (f_1^\dagger)^{b_1} (f_2^\dagger)^{b_2} \cdots (f_L^\dagger)^{b_L} |0\rangle. \quad (\text{A27})$$

[Note that the order of the factors on the right-hand side is important since they generally do not commute according to Eq. (A25).] As usual, the occupation (or particle) number operator is defined as

$$n_k := f_k^\dagger f_k. \quad (\text{A28})$$

With Eq. (A25) it follows that $n_k f_k^\dagger = f_k^\dagger - f_k^\dagger n_k$ and $n_k f_l^\dagger = f_l^\dagger n_k$ if $k \neq l$. Together with Eqs. (A26) and (A27) we thus can conclude that

$$n_k |\vec{b}\rangle = b_k |\vec{b}\rangle, \quad (\text{A29})$$

i.e., n_k indeed counts the number of particles (fermions) in state k . Moreover, we can infer from Eq. (A24) that

$$\tilde{H} |\vec{b}\rangle = \tilde{E}(\vec{b}) |\vec{b}\rangle, \quad (\text{A30})$$

$$\tilde{E}(\vec{b}) := \sum_{k=1}^L b_k \tilde{E}_k, \quad (\text{A31})$$

and that $\langle \vec{b}' | \vec{b} \rangle = \delta_{\vec{b}' \vec{b}}$, where $\delta_{\vec{b}' \vec{b}} := 1$ if $\vec{b}' = \vec{b}$ and $\delta_{\vec{b}' \vec{b}} := 0$ otherwise (generalized Kronecker delta).

In other words, we have obtained an orthonormalized set of 2^L eigenstates of \tilde{H} , i.e., we have formally solved the eigenvalue problem for any Hamiltonian \tilde{H} of the general form (A22).

Note that our present energies \tilde{E}_k and matrix elements U_{kl} have a different meaning than the energies and matrix elements appearing in Sec. II of the main paper (see in and around Eq. (4)): The latter refer to properties of the full many-body Hamiltonian, while the former refer to certain single particle properties. In particular, the many-body energies E_n in Sec. II essentially correspond to the energies $\tilde{E}(\vec{b})$ in Eq. (A31), albeit a different labeling of those energies by n and by \vec{b} , respectively, is employed in the two cases.

We finally note that any given energy eigenstate in Eq. (A27) (apart from $|0\rangle$) can be rewritten as

$$|k_1, \dots, k_n\rangle := f_{k_1}^\dagger \cdots f_{k_n}^\dagger |0\rangle \quad (\text{A32})$$

for some suitably chosen $n \in \{1, \dots, L\}$ and $k_1, \dots, k_n \in \{1, \dots, L\}$ with $k_1 < k_2 < \dots < k_n$. In the context of our Hubbard-like models from Eq. (A15) with vacuum state $|0\rangle$ (see below Eq. (A26)), such an energy eigenstate (A32) is – for obvious reasons – often denoted as “ n -particle excitation”. Exploiting Eqs. (A10), (A20), and (A23) we thus can conclude that

$$|k_1, \dots, k_n\rangle = \sum' \tau(\mathbf{l}) U_{k_1 l_1}^* \cdots U_{k_n l_n}^* \sigma_{l_1}^+ \cdots \sigma_{l_n}^+ |0\rangle, \quad (\text{A33})$$

where \sum' indicates a sum over all pairwise different indices $l_1, \dots, l_n \in \{1, \dots, L\}$, and where $\tau(\mathbf{l})$ is either $+1$ or -1 , but for the rest depends in a very complicated way on $\mathbf{l} := (l_1, \dots, l_n)$ as a consequence of Eq. (A20). Observing that all σ_l^+ commute with each other, this implies

$$|k_1, \dots, k_n\rangle = \sum'' c(l_1, \dots, l_n) \sigma_{l_1}^+ \cdots \sigma_{l_n}^+ |0\rangle, \quad (\text{A34})$$

where \sum'' indicates a sum over all $l_1, \dots, l_n \in \{1, \dots, L\}$ with $l_1 < l_2 < \dots < l_n$ and thus consists of $\binom{L}{n}$ summands. Furthermore,

$$c(l_1, \dots, l_n) := \sum_{\Pi} \tau(\Pi(\mathbf{l})) U_{k_1 l_{\Pi(1)}}^* \cdots U_{k_n l_{\Pi(n)}}^*, \quad (\text{A35})$$

where the sum is meant to run over all permutations Π of $\{1, \dots, n\}$ and thus consist of $n!$ summands. Recalling the definitions above Eq. (A26), the last factors $\sigma_{l_1}^+ \cdots \sigma_{l_n}^+ |0\rangle$ in Eq. (A34) may be viewed as “ n -spin excitations”, i.e.,

a product state where all spins with indices l_1, \dots, l_n point “up” and all other spins point “down”. Thus, the energy eigenstate on the left-hand side of Eq. (A34) amounts to a weighted sum over all possible n -spin excitations. Finally, one readily verifies that $\sigma_{l_1}^+ \cdots \sigma_{l_n}^+ |0\rangle$ is an eigenstate of the conserved quantity S^z (total spin) defined below Eq. (A1), and that the corresponding eigenvalue is given by $(2n - L)/2$. It follows that also Eq. (A34) is an eigenstate of S^z with eigenvalue $(2n - L)/2$. In conclusion, every eigenspace of S^z is spanned by all the $\binom{L}{n}$ energy eigenstates (A34) with a fixed value of n , and is invariant under the system dynamics generated by H .

3. Remaining steps

The remaining task is to explicitly determine the quantities U_{kl} and \tilde{E}_k appearing in Eqs. (A23), (A24). Moreover, we again focus on Hamiltonians (A22) of the specific form (A15), i.e., with

$$B_{kl} = -\delta_{kl+1} J_l/2 - \delta_{k+1l} J_k/2 - \delta_{kl} G_l, \quad (\text{A36})$$

for all $k, l \in \{1, \dots, L\}$.

Once this problem is solved, one can conclude from Eqs. (A6), (A30), and (A31) that

$$H |\vec{b}\rangle = E(\vec{b}) |\vec{b}\rangle, \quad (\text{A37})$$

$$E(\vec{b}) := G_{tot} + \sum_{l=1}^L b_l \tilde{E}_l. \quad (\text{A38})$$

Accordingly, it is natural to employ the eigenbasis $|\vec{b}\rangle$ of H for all the remaining calculations. To this end, it is in view of Eq. (A27) also necessary to express the considered observables in terms of the operators f_l^\dagger and f_l . For the specific observables in Eqs. (A12)-(A14) this is readily achieved by inverting Eq. (A23), yielding

$$c_l = \sum_{k=1}^L U_{kl}^* f_k, \quad (\text{A39})$$

and then introducing this relation into Eqs. (A9) and (A12)-(A14).

According to the discussion below Eq. (A22), we have to solve the eigenvalue problem $BU^\dagger = U^\dagger D$. On the level of the matrix elements, this amounts to L^2 equations of the form

$$\sum_j B_{lj} U_{kj}^* = \sum_j U_{jl}^* D_{jk} = U_{kl}^* \tilde{E}_k \quad (\text{A40})$$

for arbitrary $k, l \in \{1, \dots, L\}$.

To simplify the notation, let us temporarily consider $k \in \{1, \dots, L\}$ as arbitrary but fixed, and employ the abbreviations

$$E := \tilde{E}_k, \quad (\text{A41})$$

$$a_l := \kappa U_{kl}^*. \quad (\text{A42})$$

Moreover, while the U_{kl} are normalized according to $\sum_l |U_{kl}|^2 = 1$, we do not require such a normalization condition for the a_l 's. This is accounted for by the still arbitrary proportionality constant $\kappa \in \mathbb{C}$ in Eq. (A42). Our only requirement is that $\kappa \neq 0$, or equivalently, that at least one of the a_l 's must be non-zero. Introducing Eqs. (A36), (A41), and (A42) into Eq. (A40) then yields

$$\bar{\delta}_{lL} J_l a_{l+1} + \bar{\delta}_{l1} J_{l-1} a_{l-1} = -2(E + G_l) a_l \quad (\text{A43})$$

for all $l = 1, \dots, L$, where $\bar{\delta}_{lj} := 1 - \delta_{lj}$ is the complementary Kronecker delta (hence the quantities J_0, J_L, a_0 , and a_{L+1} , which appear in Eq. (A43) when $l = 1$ or $l = L$ but have not been specified until now, actually do not matter).

In summary, we are left with the task to determine L linearly independent solutions of the L coupled linear equations (A43). The energies \tilde{E}_k and matrix elements U_{kl} then readily follow as detailed in and around Eqs. (A41), (A42).

Note that for any given solution a_l of Eq. (A43), also the real- and imaginary-parts of a_l will be solutions. It follows that, if it is convenient, we always may assume without loss of generality that the a_l and hence the U_{kl} are purely real quantities.

4. Explicit solution for the model from Eq. (7)

For general models of the form (A1), an explicit analytical solution of the remaining problem from the second-to-last paragraph of the previous subsection is still a quite demanding task. However, for the actual model of interest in our present paper, see Eq. (7), the solution is straightforward. The details are as follows.

Our present special case from Eq. (7) corresponds to $J_l = J$ and $G_l = G$ for all l in Eq. (A1), hence Eq. (A43) takes the form

$$J(a_{l+1} + a_{l-1}) = -2(E + G) a_l \text{ for } l = 2, \dots, L-1, \quad (\text{A44})$$

$$J a_2 = -2(E + G) a_1, \quad (\text{A45})$$

$$J a_{L-1} = -2(E + G) a_L. \quad (\text{A46})$$

One readily verifies by inspection that the L linearly independent solutions of these equations (see also in and around Eqs. (A41), (A42)) are given by

$$\tilde{E}_k = -J \cos(k\pi/(L+1)) - G, \quad (\text{A47})$$

$$U_{kl} = \sqrt{\frac{2}{L+1}} \sin(lk\pi/(L+1)) =: \tilde{S}_k^l. \quad (\text{A48})$$

In particular, one readily verifies that the normalization condition $\sum_{k=1}^L (\tilde{S}_k^l)^2 = 1$ is fulfilled for any $l \in \{1, \dots, L\}$. By means of a more involved calculation, one also can verify explicitly that, as it must be, the orthonormality conditions $\sum_{k=1}^L \tilde{S}_k^l \tilde{S}_k^j = \delta_{jl}$ and $\sum_{k=1}^L \tilde{S}_l^k \tilde{S}_j^k = \delta_{jl}$ are fulfilled for all $j, l \in \{1, \dots, L\}$.

5. Exponential degeneracies of the many-body energies and energy gaps

As pointed out below Eq. (A31), the set of all many-body energies E_n appearing in Eq. (4) can be identified with the set of all $\tilde{E}(\vec{b})$ in Eq. (A31), where \vec{b} is defined above Eq. (A27). [Both sets represent the spectrum of the considered many-body Hamiltonian H .] More precisely speaking, they are given by the set of all $E(\vec{b})$ in Eq. (A38), which differ from the $\tilde{E}(\vec{b})$ by a trivial constant, see also Eqs. (A6), (A30), (A37).

To begin with, we show that the Hamiltonian from Eq. (7) must exhibit many degeneracies for large L , meaning that $E_n = E_m$ for many $n \neq m$, or equivalently, $E(\vec{b}) = E(\vec{b}')$ for many $\vec{b} \neq \vec{b}'$. Let us therefore consider an arbitrary but fixed $k \in \{1, \dots, L\}$ and define $\bar{k} := L + 1 - k$. Focusing on cases with $k \neq \bar{k}$ and observing that $\cos(\pi\bar{k}/(L+1)) = -\cos(\pi k/(L+1))$, we can conclude from Eq. (A47) that

$$\tilde{E}_k + \tilde{E}_{\bar{k}} = -2G. \quad (\text{A49})$$

Next we choose two indices $j, k \in \{1, \dots, L\}$ with the property that the four numbers j, \bar{j}, k, \bar{k} are pairwise distinct. Then, the components of $\vec{b} = (b_1, \dots, b_L)$ are chosen such that $b_j = b_{\bar{j}} = 1$ and $b_k = b_{\bar{k}} = 0$, while all other s_l are arbitrary (but fixed). Similarly, the components of $\vec{b}' = (b'_1, \dots, b'_L)$ are chosen such that $b'_j = b'_{\bar{j}} = 0$, $b'_k = b'_{\bar{k}} = 1$, and $b'_l = b_l$ for all other indices l . As a consequence, one readily can infer from Eqs. (A38) and (A49) that $E(\vec{b}) = E(\vec{b}')$. In other words, each \vec{b} of the above specified structure gives rise to a pair of degenerate energies. For large L there are very many \vec{b} of this type, hence there must be a large number of degeneracies. In fact, one readily sees that their number grows exponentially with the system size L . We remark that in the special case $G = 0$ there also exist considerably simpler examples of vectors \vec{b} and \vec{b}' with the properties $\vec{b} \neq \vec{b}'$ and $E(\vec{b}) = E(\vec{b}')$.

To arrive at this conclusion, we exploited the result (A47), which in turn is only valid for the specific Hamiltonians from Eq. (7). Next, we admit the more general Hamiltonians from Eq. (A1) and we show that they must exhibit many degenerate energy gaps for large L , meaning that $E_m - E_n = E_{m'} - E_{n'}$ for many m, n, m', n' with $n \neq m$ and $(m', n') \neq (m, n)$. Equivalently, we can and will show that $E(\vec{b}) - E(\vec{b}') = E(\vec{r}) - E(\vec{r}')$ for many $\vec{b}, \vec{b}', \vec{r}, \vec{r}'$ with $\vec{b}' \neq \vec{b}$ and $(\vec{r}, \vec{r}') \neq (\vec{b}, \vec{b}')$. Let us therefore consider any $\vec{b} := (b_1, \dots, b_L)$ with $b_1 = 1$ and $b_2, \dots, b_L \in \{0, 1\}$ arbitrary but fixed. Hence, there are 2^{L-1} possible such choices of \vec{b} . For an arbitrary but fixed such \vec{b} , we choose $\vec{b}' := (b'_1, \dots, b'_L)$ with $b'_1 = 0$ and $b'_l = b_l$ for $l = 2, \dots, L$. It follows with Eq. (A38) that the energy gap $E(\vec{b}) - E(\vec{b}')$ equals E_1 . Thus, there are 2^{L-1} different pairs (\vec{b}, \vec{b}') with the same energy gap $E(\vec{b}) - E(\vec{b}')$. In other words, the maximal degeneracy of the energy

gaps is lower bounded by 2^{L-1} , and thus grows exponentially with the system size L . (Note that a faster than exponential growth is impossible since the number of all gaps only grows exponentially.)

Appendix B: Dynamical correlation functions

Similar results as we will derive them here can be found for instance in Refs. [31, 39–41]. However, the derivation itself is much harder to find in the literature.

As in the previous Appendix, we consider the generalized XX-model from Eq. (A1). As in Eq. (A27), we define $\vec{b} := (b_1, \dots, b_L)$ with $b_l \in \{0, 1\}$ and

$$|\vec{b}\rangle := (f_1^\dagger)^{b_1} (f_2^\dagger)^{b_2} \dots (f_L^\dagger)^{b_L} |0\rangle, \quad (\text{B1})$$

implying (see Eqs. (A37) and (A38))

$$H |\vec{b}\rangle = E(\vec{b}) |\vec{b}\rangle, \quad (\text{B2})$$

$$E(\vec{b}) := G_{tot} + \sum_{l=1}^L b_l \tilde{E}_l. \quad (\text{B3})$$

Accordingly, it is natural to employ the eigenbasis $|\vec{b}\rangle$ of H for all the subsequent calculations. To deal with the specific observables in Eqs. (A9) and (A12)-(A14) we additionally need the relation (see (A39))

$$c_l = \sum_{k=1}^L U_{kl}^* f_k. \quad (\text{B4})$$

As in the main paper, the canonical ensemble is defined as

$$\rho_{can} := Z^{-1} e^{-\beta H}, \quad (\text{B5})$$

$$Z := \text{tr}\{e^{-\beta H}\}, \quad (\text{B6})$$

and the corresponding thermal expectation values are abbreviated as

$$\langle A \rangle_{th} := \text{tr}\{\rho_{can} A\}. \quad (\text{B7})$$

Utilizing the basis $|\vec{b}\rangle$ to evaluate the traces in Eqs. (B6) and (B7) we thus obtain

$$\langle A \rangle_{th} = Z^{-1} \sum_{\vec{b}} e^{-\beta E(\vec{b})} \langle \vec{b} | A | \vec{b} \rangle, \quad (\text{B8})$$

$$Z = \sum_{\vec{b}} e^{-\beta E(\vec{b})}, \quad (\text{B9})$$

where

$$\sum_{\vec{b}} := \sum_{b_1=0}^1 \sum_{b_2=0}^1 \dots \sum_{b_L=0}^1 \quad (\text{B10})$$

denotes the sum over all the 2^L possible vectors $\vec{b} := (b_1, \dots, b_L)$ with $b_l \in \{0, 1\}$.

Finally (and as in the main paper),

$$A(t) := e^{iHt} A e^{-iHt} \quad (\text{B11})$$

represents the observable A at time t in the Heisenberg picture.

In the following, the same definitions as in Eqs. (B7) and (B11) will also be adopted for arbitrary (not necessarily Hermitian) operators A .

A particularly important example will turn out to be the (non-Hermitian) operator $A = f_l$, yielding with Eq. (B11) the relation

$$\dot{f}_l(t) = i e^{iHt} [H, f_l] e^{-iHt}. \quad (\text{B12})$$

With Eqs. (A6) and (A24) we can conclude that

$$[H, f_l] = \sum_{k=1}^L \tilde{E}_k [f_k^\dagger f_k, f_l]. \quad (\text{B13})$$

From the basic anti-commutation relations (A25) one can infer that $[f_k^\dagger f_k, f_k] = -f_k$ and $[f_k^\dagger f_k, f_l] = 0$ if $k \neq l$, implying $[H, f_l] = -\tilde{E}_l f_l$. Together with Eq. (B12) this yields $\dot{f}_l(t) = -i\tilde{E}_l f_l(t)$ and thus

$$f_l(t) = e^{-i\tilde{E}_l t} f_l. \quad (\text{B14})$$

1. Evaluation of $\langle \sigma_i^z \sigma_j^z(t) \rangle_{\text{th}}$ and $C_{s_i^z s_j^z}(t)$

As a first example, let us consider temporal correlations of the form $\langle \sigma_i^z \sigma_j^z(t) \rangle_{\text{th}}$, where $\sigma_i^z = 2c_l^\dagger c_l - 1$ according to Eq. (A14). With Eq. (B11) it follows that $\sigma_i^z(t) = 2c_l(t)^\dagger c_l(t) - 1$ and with Eqs. (B5)-(B11) that $\langle c_l(t)^\dagger c_l(t) \rangle_{\text{th}} = \langle c_l^\dagger c_l \rangle_{\text{th}}$ independent of t . We thus can conclude that

$$\langle \sigma_i^z \sigma_j^z(t) \rangle_{\text{th}} = 4B(t) + R, \quad (\text{B15})$$

$$B(t) := \langle c_l^\dagger c_l c_j^\dagger c_j(t) \rangle_{\text{th}}, \quad (\text{B16})$$

$$R := 1 - 2\langle c_l^\dagger c_l \rangle_{\text{th}} - 2\langle c_j^\dagger c_j \rangle_{\text{th}}. \quad (\text{B17})$$

Employing Eq. (B4) it follows that

$$\langle c_l^\dagger c_l \rangle_{\text{th}} = \sum_{k_1, k_2=1}^L U_{k_1 l} U_{k_2 l}^* \langle f_{k_1}^\dagger f_{k_2} \rangle_{\text{th}}. \quad (\text{B18})$$

Similarly, Eqs. (B4) and (B14) imply

$$B(t) = \sum_{\mathbf{k}} U_{k_1 l} U_{k_2 l}^* U_{k_3 j} U_{k_4 j}^* e^{i(\tilde{E}_{k_3} - \tilde{E}_{k_4})t} B_{\mathbf{k}}, \quad (\text{B19})$$

$$B_{\mathbf{k}} := \langle f_{k_1}^\dagger f_{k_2} f_{k_3}^\dagger f_{k_4} \rangle_{\text{th}}, \quad (\text{B20})$$

where $\mathbf{k} := (k_1, k_2, k_3, k_4)$ and the sum in Eq. (B19) runs over all $k_1, \dots, k_4 \in \{1, \dots, L\}$.

The last term in Eq. (B18) can be rewritten by means of Eq. (B8) as

$$\langle f_{k_1}^\dagger f_{k_2} \rangle_{\text{th}} = Z^{-1} \sum_{\vec{b}} e^{-\beta E(\vec{b})} \langle \vec{b} | f_{k_1}^\dagger f_{k_2} | \vec{b} \rangle. \quad (\text{B21})$$

Taking into account the basic relations (A25), (A26), and (B1), a straightforward but somewhat tedious calculation shows that $\langle \vec{b} | f_{k_1}^\dagger f_{k_2} | \vec{b} \rangle$ must vanish unless $k_1 = k_2$.

The following alternative line of reasoning is intuitively more appealing (but actually working out all the details is about equally laborious): From the discussion below Eq. (A42) it follows that we still have the freedom to replace all U_{kl} by $e^{i\alpha_k} U_{kl}$, where α_k are arbitrary (real-valued) phases, without changing any physical properties of the system, for instance the left-hand side of Eq. (B18). Moreover, it can be shown that also the quantities $\langle f_{k_1}^\dagger f_{k_2} \rangle_{\text{th}}$ on the right-hand side of Eq. (B18) must be independent of those phases. The latter claim is obvious as far as the quantities Z^{-1} and $e^{-\beta E(\vec{b})}$ in Eq. (B8) are concerned. With respect to the remaining quantities $\langle \vec{b} | f_{k_1}^\dagger f_{k_2} | \vec{b} \rangle$ our claim follows from the fact that neither in the definition of $|\vec{b}\rangle$ from Eq. (B1) nor in the basic anti-commutation relations in Eq. (A25) those phases play any role. It is thus quite reasonable to expect that the independence from all those extra factors $e^{i(\alpha_{k_1} - \alpha_{k_2})}$ on the right-hand side Eq. (B18) implies that all summands with $k_1 \neq k_2$ must be zero. A more formal verification follows by exploiting that all mixed second derivatives $\partial^2 / \partial \alpha_{k_1} \partial \alpha_{k_2}$ of Eq. (B18) must vanish.

From Eqs. (A29) and (A28) it moreover follows that $\langle \vec{b} | f_k^\dagger f_k | \vec{b} \rangle = \langle \vec{b} | n_k | \vec{b} \rangle = b_k$. Together with Eq. (B9) we thus can rewrite Eq. (B18) as

$$\langle c_l^\dagger c_l \rangle_{\text{th}} = \sum_{k=1}^L |U_{kl}|^2 p_k, \quad (\text{B22})$$

$$p_k := \frac{\sum_{\vec{b}} b_k e^{-\beta E(\vec{b})}}{\sum_{\vec{b}} e^{-\beta E(\vec{b})}}. \quad (\text{B23})$$

Exploiting Eqs. (B3) and (B10), the denominator in Eq. (B23) can be rewritten as

$$\sum_{\vec{b}} e^{-\beta E(\vec{b})} = e^{-\beta G_{\text{tot}}} \prod_{l=1}^L z_l, \quad (\text{B24})$$

$$z_l := \sum_{b_l=0}^1 e^{-\beta b_l \tilde{E}_l}. \quad (\text{B25})$$

Likewise, the numerator in Eq. (B23) can be written in almost the same form as in Eq. (B24), except that the factor z_k must now be replaced by

$$\tilde{z}_k := \sum_{b_k=0}^1 b_k e^{-\beta b_k \tilde{E}_k}. \quad (\text{B26})$$

Altogether, this yields

$$p_k = \frac{\tilde{z}_k}{z_k} = \frac{\sum_{b_k=0}^1 b_k e^{-\beta b_k \tilde{E}_k}}{\sum_{b_k=0}^1 e^{-\beta b_k \tilde{E}_k}} = \frac{e^{-\beta \tilde{E}_k}}{1 + e^{-\beta \tilde{E}_k}}. \quad (\text{B27})$$

Hence, Eq. (B22) can be rewritten as

$$\langle c_l^\dagger c_l \rangle_{\text{th}} = \sum_{k=1}^L |U_{kl}|^2 f(\tilde{E}_k), \quad (\text{B28})$$

where

$$f(E) := \frac{1}{e^{\beta E} + 1} \quad (\text{B29})$$

is the Fermi function.

The evaluation of Eqs. (B19) and (B20) is in principle similar but in detail more involved. In particular, Eq. (B20) is again found to vanish unless each of the two creation operators has a ‘‘partner’’ with identical index among the two annihilation operators (see also the intuitive arguments below Eq. (B21)). More precisely speaking, there remain three types of possibly non-vanishing contributions. (i) $k_1 = k_2 = k_3 = k_4$. (ii) $k_1 = k_2$ and $k_3 = k_4$ and $k_1 \neq k_3$ (or, equivalently, $k_1 \neq k_4$). (iii) $k_1 = k_4$ and $k_2 = k_3$ and $k_1 \neq k_2$. Note that the extra conditions $k_1 \neq k_3$ in (ii) and $k_1 \neq k_2$ in (iii) are needed to make sure that each possibly non-vanishing contribution is contained in one and only one of the three subsets (i)-(iii).

The further steps are similar as in Eqs. (B22)-(B29) and therefore not explained in detail. In case (i) one finds (setting $k := k_1$) that

$$\langle \vec{b} | f_k^\dagger f_k f_k^\dagger f_k | \vec{b} \rangle = \langle \vec{b} | n_k^2 | \vec{b} \rangle = b_k^2 = b_k \quad (\text{B30})$$

and thus $B_{\mathbf{k}} = f(\tilde{E}_k)$. In case (ii) one finds that

$$\langle \vec{b} | f_{k_1}^\dagger f_{k_1} f_{k_3}^\dagger f_{k_3} | \vec{b} \rangle = \langle \vec{b} | n_{k_1} n_{k_3} | \vec{b} \rangle = b_{k_1} b_{k_3} \quad (\text{B31})$$

and thus $B_{\mathbf{k}} = f(\tilde{E}_{k_1})f(\tilde{E}_{k_3})$. In case (iii) one finds that

$$\begin{aligned} \langle \vec{b} | f_{k_1}^\dagger f_{k_2} f_{k_2}^\dagger f_{k_1} | \vec{b} \rangle &= \langle \vec{b} | f_{k_1}^\dagger f_{k_1} (1 - f_{k_2}^\dagger f_{k_2}) | \vec{b} \rangle \\ &= \langle \vec{b} | n_{k_1} (1 - n_{k_2}) | \vec{b} \rangle = b_{k_1} (1 - b_{k_2}) \end{aligned} \quad (\text{B32})$$

and thus $B_{\mathbf{k}} = f(\tilde{E}_{k_1})[1 - f(\tilde{E}_{k_2})]$.

Accordingly, Eq. (B19) can be rewritten as

$$B(t) = B^{(i)} + B^{(ii)} + B^{(iii)}(t), \quad (\text{B33})$$

$$B^{(i)} := \sum_{k=1}^L |U_{kl}|^2 |U_{kj}|^2 f(\tilde{E}_k), \quad (\text{B34})$$

$$\begin{aligned} B^{(ii)} &:= \sum_{k_1, k_3=1}^L |U_{k_1 l}|^2 |U_{k_3 j}|^2 f(\tilde{E}_{k_1}) f(\tilde{E}_{k_3}) \\ &\quad - \sum_{k=1}^L |U_{kl}|^2 |U_{kj}|^2 [f(\tilde{E}_k)]^2, \end{aligned} \quad (\text{B35})$$

$$\begin{aligned} B^{(iii)}(t) &:= \sum_{k_1, k_2=1}^L U_{k_1 l} U_{k_2 l}^* U_{k_2 j} U_{k_1 j}^* e^{i(\tilde{E}_{k_2} - \tilde{E}_{k_1})t} \\ &\quad \times f(\tilde{E}_{k_1}) [1 - f(\tilde{E}_{k_2})] \\ &\quad - \sum_{k=1}^L |U_{kl}|^2 |U_{kj}|^2 f(\tilde{E}_k) [1 - f(\tilde{E}_k)] \end{aligned} \quad (\text{B36})$$

The last sum in Eq. (B35) has its origin in the fact that $k_1 = k_3$ has been excluded in case (ii), and likewise for the last sum in Eq. (B36).

Our first observation is that the contributions to Eqs. (B33) by Eq. (B34) and by the last sums in Eqs. (B35) and (B36) cancel each other, i.e., only the first sums in Eqs. (B35) and (B36) remain. Second, the first sum in Eq. (B35) can be rewritten by means of Eq. (B28) as $\langle c_l^\dagger c_l \rangle_{\text{th}} \langle c_j^\dagger c_j \rangle_{\text{th}}$. Finally, in the first sum in Eq. (B36) we can exploit that

$$1 - f(E) = f(-E) \quad (\text{B37})$$

according to Eq. (B29). Altogether, we thus obtain

$$B(t) = \langle c_l^\dagger c_l \rangle_{\text{th}} \langle c_j^\dagger c_j \rangle_{\text{th}} + \mathcal{B}_{lj}^+(t) [\mathcal{B}_{lj}^-(t)]^*, \quad (\text{B38})$$

$$\mathcal{B}_{lj}^\pm(t) := \sum_{k=1}^L U_{kl} U_{kj}^* e^{-i\tilde{E}_k t} f(\pm \tilde{E}_k). \quad (\text{B39})$$

Since $\sigma_l^z = 2c_l^\dagger c_l - 1$ (see below Eq. (B14)) and $s_l^a = \sigma_l^a/2$ (see paragraph before Eq. (A2)) we can infer from Eq. (B28) that

$$\langle s_l^z \rangle_{\text{th}} = \sum_{k=1}^L |U_{kl}|^2 f(\tilde{E}_k) - 1/2 \quad (\text{B40})$$

for all $l \in \{1, \dots, L\}$. By exploiting the definition of $f(E)$ in Eq. (B29) and the property $\sum_{l=1}^L |U_{jl}|^2 = 1$ (see below Eq. (A48)) this yields

$$\langle s_l^z \rangle_{\text{th}} = \frac{1}{2} \sum_{k=1}^L |U_{kl}|^2 \tanh(-\beta \tilde{E}_k / 2). \quad (\text{B41})$$

Likewise, upon adopting the definition (13) for the dynamical correlation function $C_{VA}(t)$ of two arbitrary operators V and A we can conclude from Eqs. (B15)-(B17) and (B38) that

$$C_{s_l^z s_j^z}(t) = \mathcal{B}_{lj}^+(t) [\mathcal{B}_{lj}^-(t)]^* \quad (\text{B42})$$

for all $l, j \in \{1, \dots, L\}$.

2. Evaluation of more general temporal correlations

As a second example, we consider the observables σ_l^x , see Eqs. (A12), (A16), and (B4). Similarly as above Eq. (B22) and around Eq. (B30), one finds after a few steps that we have to evaluate sums of expressions of the form $\langle \vec{b} | O | \vec{b} \rangle$, where O is always a product of an odd number of creation and annihilation operators. As a consequence (see also the intuitive arguments below Eq. (B21)), all those expressions $\langle \vec{b} | O | \vec{b} \rangle$ must be zero, implying $\langle \sigma_l^x \rangle_{\text{th}} = 0$. Analogous conclusions apply to σ_l^y , and hence

$$\langle s_l^{x,y} \rangle_{\text{th}} = 0 \quad (\text{B43})$$

for all $l \in \{1, \dots, L\}$. The same result can also be derived by means of symmetry considerations, see the Supplemental Material of Ref. [36].

Analogously one finds that temporal correlations of the form $\langle \sigma_l^z \sigma_j^x(t) \rangle_{\text{th}}$ give rise exclusively to odd numbers of creation and annihilation operators, resulting in

$$C_{s_l^z s_j^x}(t) = 0 \quad (\text{B44})$$

for all $l, j \in \{1, \dots, L\}$.

Finally, temporal correlations of the form $\langle \sigma_l^a \sigma_j^b(t) \rangle_{\text{th}}$ with $a, b \in \{x, y\}$ turn out to be in general considerably more difficult to evaluate. The reason is the factor Z_l from Eqs. (A9) or (A16) appearing in Eqs. (A12) and (A13). An exception is the case $l = j = 1$ (since $Z_1 = 1$). Omitting the details, the final result is

$$C_{s_1^x s_1^x}(t) = C_{s_1^y s_1^y}(t) = \frac{\mathcal{B}_{11}^+(t) + [\mathcal{B}_{11}^-(t)]^*}{4}, \quad (\text{B45})$$

$$C_{s_1^y s_1^x}(t) = -C_{s_1^x s_1^y}(t) = \frac{\mathcal{B}_{11}^+(t) - [\mathcal{B}_{11}^-(t)]^*}{4i}, \quad (\text{B46})$$

where $\mathcal{B}_{11}^\pm(t)$ is defined in Eq. (B39), i.e.,

$$\mathcal{B}_{11}^\pm(t) = \sum_{k=1}^L |U_{k1}|^2 e^{-i\tilde{E}_k t} f(\pm\tilde{E}_k). \quad (\text{B47})$$

Appendix C: Explicit evaluation of Eq. (14) for specific examples

Our first examples are perturbations V and observables A of the form

$$V = s_\nu^z, \quad A = s_\alpha^z \quad (\text{C1})$$

with $\nu, \alpha \in \{1, \dots, L\}$ arbitrary but fixed. Exploiting Eqs. (B42) and (B39) it follows that

$$C_{s_\nu^z s_\alpha^z}(t) = \sum_{m,n=1}^L U_{mn}^{\nu\alpha} \tilde{f}_{mn} e_{mn}(t), \quad (\text{C2})$$

$$U_{mn}^{\nu\alpha} := U_{m\nu} U_{m\alpha}^* U_{n\nu}^* U_{n\alpha}, \quad (\text{C3})$$

$$\tilde{f}_{mn} := f(\tilde{E}_m) f(-\tilde{E}_n), \quad (\text{C4})$$

$$e_{mn}(t) := e^{-i(\tilde{E}_m - \tilde{E}_n)t}, \quad (\text{C5})$$

and with Eq. (14) that

$$\langle s_\alpha^z \rangle_t - \langle s_\alpha^z \rangle_{\text{th}} = g\beta \sum_{m,n=1}^L U_{mn}^{\nu\alpha} \tilde{f}_{mn} e_{mn}(t), \quad (\text{C6})$$

$$f_{mn} := \tilde{f}_{mn} Q_{mn}, \quad (\text{C7})$$

$$Q_{mn} := \sum_{k=0}^{\infty} \frac{(\beta(\tilde{E}_m - \tilde{E}_n))^k}{(k+1)!}. \quad (\text{C8})$$

We thus can conclude that

$$Q_{mn} = F(\beta(\tilde{E}_m - \tilde{E}_n)), \quad (\text{C9})$$

$$F(x) := \sum_{k=0}^{\infty} \frac{x^k}{(k+1)!} = \frac{e^x - 1}{x}. \quad (\text{C10})$$

Furthermore, the quantity f_{mn} from Eq. (C7) can be rewritten by means of Eqs. (B29), (C4), (C9), (C10) as

$$\begin{aligned} f_{mn} &= \frac{\sinh\left(\beta \frac{\tilde{E}_m - \tilde{E}_n}{2}\right)}{2\beta(\tilde{E}_m - \tilde{E}_n)} \frac{1}{\cosh\left(\beta \frac{\tilde{E}_m}{2}\right) \cosh\left(\beta \frac{\tilde{E}_n}{2}\right)} \\ &= \frac{\tanh\left(\beta \frac{\tilde{E}_m}{2}\right) - \tanh\left(\beta \frac{\tilde{E}_n}{2}\right)}{2\beta(\tilde{E}_m - \tilde{E}_n)}. \end{aligned} \quad (\text{C11})$$

A more detailed discussion of this quantity is provided in Appendix D. Introducing Eqs. (A47) and (A48) into these results, one readily recovers Eq. (17).

In passing we note that the following properties of Eq. (C6), which we also mentioned in the main text for the specific model considered therein, are in fact generally valid. The starting point is the observation at the end of Sec. A 4 that all U_{kl} may be assumed to be real-valued. It follows that the $U_{mn}^{\nu\alpha}$ in Eq. (C3) are real-valued, implying that Eq. (C6) is symmetric with respect to the indices ν and α . Moreover, Eq. (C3) as well as Eq. (C11) are symmetric with respect to m and n . Upon interchanging the summation indices m and n in Eq. (C6) one thus can conclude that the entire sum must be real-valued, and that it must be time-inversion invariant. Finally, Eq. (C11) is obviously an even function of β , hence the same property is inherited by Eq. (C6).

As our next examples we consider perturbations V and observables A of the form $V = A = s_1^a$ with $a \in \{x, y\}$. In this case, upon exploiting Eqs. (B45) and (B47) one readily arrives by similar (but simpler) calculations as above at the result (78) in the main paper.

Likewise, for examples of the form $V = s_1^y$ and $A = s_1^x$ one may exploit Eq. (B46) to recover the result (79). Finally, the case $V = s_1^x$ and $A = s_1^y$ simply amounts to a sign change compared to the former case according to Eq. (B46).

Appendix D: Properties of f_{mn}

We rewrite Eq. (19) as

$$f_{mn} = g(\beta(\tilde{E}_m - \tilde{E}_n)/2, \beta\tilde{E}_n/2)/4, \quad (\text{D1})$$

$$g(x, y) := \frac{\tanh(x+y) - \tanh(y)}{x}. \quad (\text{D2})$$

Considering y as arbitrary but fixed, Taylor's theorem implies

$$\tanh(x+y) = \tanh(y) + x \tanh'(\xi) \quad (\text{D3})$$

for some ξ which in general depends on x and y but which is known to always take a value between y and $x+y$. Since $\tanh'(\xi) = 1/\cosh^2(\xi) \in (0, 1]$ for all $\xi \in \mathbb{R}$ it follows by introducing Eq. (D3) into Eq. (D2) that $0 < g(x, y) \leq 1$ for all $x, y \in \mathbb{R}$ and with Eq. (D1) that

$$0 < f_{mn} \leq 1/4 \quad (\text{D4})$$

for all m, n . Furthermore, if $|x| \ll 1$ it follows that $g(x, y) \simeq 1/\cosh^2(y)$, implying the approximation

$$f_{mn} \simeq \frac{1}{4 \cosh^2(\beta \tilde{E}_n/2)} \text{ if } |\beta(\tilde{E}_m - \tilde{E}_n)| \ll 1. \quad (\text{D5})$$

Likewise, considering the limit $x \rightarrow 0$ one can infer (without any approximation) that

$$f_{nn} = \frac{1}{4 \cosh^2(\beta \tilde{E}_n/2)} \quad (\text{D6})$$

for all n .

While all so far considerations are valid for general models of the form (A1), let us finally focus on the model of actual interest in the main paper, see Eq. (7), for which the energies \tilde{E}_n are given by Eq. (21). As in Sec. IV C we furthermore focus on the case

$$|\beta J| \ll 1. \quad (\text{D7})$$

In view of Eq. (21) it follows that $|\beta(\tilde{E}_m - \tilde{E}_n)| \ll 1$ for all m, n , and that $\cosh(\beta \tilde{E}_n/2) \simeq \cosh(\beta Gh/2)$ for all n . Together with Eq. (D5) we thus arrive at the approximation

$$f_{mn} \simeq \frac{1}{4 \cosh^2(\beta G/2)} \quad (\text{D8})$$

for all m, n . Moreover, it is straightforward to verify that the relative error of this approximation is at most of the order of $|\beta J|$.

Appendix E: Evaluation and discussion of $\langle s_l^z \rangle_{\text{th}}$

While most of the considerations in the previous Appendices A-D are valid for general models of the form (A1), we will focus in this Appendix on the specific XX-model from Eq. (7) of the main paper. Hence, we can utilize the explicit solutions obtained in Sec. A 4.

Recalling the property $\sum_{l=1}^L |U_{jl}|^2 = 1$ (see below Eq. (A48)) we can infer from Eq. (B41) that (as expected)

$$\langle s_l^z \rangle_{\text{th}} \in [-1/2, 1/2]. \quad (\text{E1})$$

Furthermore, by exploiting Eqs. (A47) and (A48) we can rewrite Eq. (B41) as

$$\langle s_l^z \rangle_{\text{th}} = F(\beta J/2, \beta G/2)/(L+1), \quad (\text{E2})$$

$$F(x, y) := \sum_{k=1}^L \sin^2(\varphi_k l) \tanh(x \cos(\varphi_k) + y), \quad (\text{E3})$$

$$\varphi_k := \pi k/(L+1). \quad (\text{E4})$$

Similarly as below Eq. (24), upon replacing all indices k in Eq. (E3) by $L+1-k$ one can infer that $F(x, y) = F(-x, y)$. Furthermore, it is obvious that $F(-x, -y) = -F(x, y)$, and, by combining both relations, that $F(x, -y) = -F(x, y)$.

Altogether we thus can conclude that $\langle s_l^z \rangle_{\text{th}}$ in Eq. (E1) must be an even function of J , and an odd function of β and of G . In particular,

$$\langle s_l^z \rangle_{\text{th}} = 0 \text{ if } G = 0 \text{ or } \beta = 0. \quad (\text{E5})$$

Turning to asymptotically large G , and assuming that $\beta > 0$, Eq. (A47) implies $\beta \tilde{E}_k \rightarrow -\infty$. Together with Eq. (B41) it follows that

$$\langle s_l^z \rangle_{\text{th}} \rightarrow 1/2 \text{ if } \beta > 0 \text{ and } G \rightarrow \infty, \quad (\text{E6})$$

and symmetrically (see above) for $G \rightarrow -\infty$ or $\beta < 0$.

Finally, we focus on the case

$$|\beta J| \ll 1. \quad (\text{E7})$$

Expanding Eq. (E3) up to the second order in x , a straightforward but somewhat lengthy calculation then yields

$$\langle s_l^z \rangle_{\text{th}} = \frac{1}{2} \tanh\left(\frac{\beta G}{2}\right) [1 - (\beta J)^2 \gamma + \mathcal{O}((\beta J)^4)], \quad (\text{E8})$$

$$\gamma := \frac{L}{L+1} \frac{2 - \delta_{l1} - \delta_{lL}}{4 \cosh^2(\frac{\beta G}{2})}, \quad (\text{E9})$$

where δ_{lj} is the Kronecker delta. Most notably, the sites with $l = 1$ and $l = L$ thus exhibit in general a different behavior than the rest of the chain. It seems reasonable to expect that also the sites with $l = 2$ and $l = L - 1$ will exhibit such differences in fourth order of βJ , and so on.

Appendix F: Some properties of $J_k(t)$

Focusing on Bessel functions of the first kind $J_k(t)$ with $k \in \mathbb{N}_0$, their series expansion assumes the form (see (9.1.10) in [37])

$$J_k(t) = (t/2)^k \sum_{n=0}^{\infty} \frac{(-t^2/4)^n}{n!(n+k)!}. \quad (\text{F1})$$

Approximations for small t can thus be readily inferred.

For sufficiently large t it is known (see (9.2.5), (9.2.8)-(9.2.10) in [37]) that

$$J_k(t) = \sqrt{\frac{2}{\pi t}} [q_k(t) \cos(t - \phi_k) - r_k(t) \sin(t - \phi_k)], \quad (\text{F2})$$

$$\phi_k := \pi k/2 + \pi/4, \quad (\text{F3})$$

$$q_k(t) := \sum_{n=0}^{\infty} (-1)^n \frac{c_k(2n)}{t^{2n}}, \quad (\text{F4})$$

$$r_k(t) := \sum_{n=0}^{\infty} (-1)^n \frac{c_k(2n+1)}{t^{2n+1}}, \quad (\text{F5})$$

$$c_k(0) := 1, \quad (\text{F6})$$

$$c_k(n) := \frac{(\kappa - 1^2)(\kappa - 3^2) \cdots (\kappa - (2n - 1)^2)}{8^n n!}, \quad (\text{F7})$$

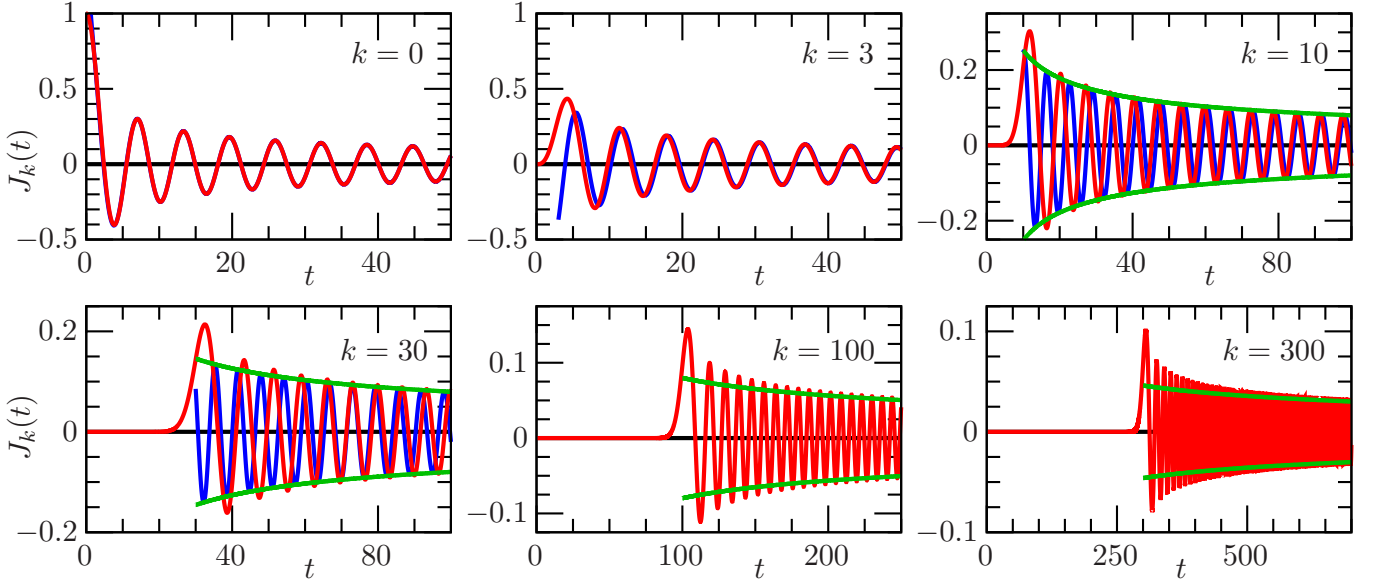


FIG. 12. Red: The Bessel functions $J_k(t)$ for $k = 0, 3, 10, 30, 100, 300$. Note the different scalings of the axes. Blue: the large- t asymptotics from Eq. (F8) for $t \geq k$. Green: The envelopes $\pm\sqrt{2\pi/t}$ of the damped (blue) oscillations from Eq. (F8). For $k = 0$ the blue curve is almost completely covered by the red curve. With increasing k , the convergence of the blue towards the red curves takes longer and longer, in agreement with the convergence criterion below Eq. (F8). For $k = 30$ this convergence is already far outside the plotted range. For $k = 100$ and $k = 300$ the convergence is reached even much later, hence the blue curves have been omitted altogether. On the other hand, the envelopes of the damped red and blue oscillations converge much earlier than the frequencies for large k .

where $\kappa := 4k^2$ and $n \geq 1$ in Eq. (F7). More precisely speaking, the remainder after n terms in the expansions (F4), (F5) does not exceed the $n + 1$ -th term in absolute value. It follows that

$$J_k(t) \simeq \sqrt{\frac{2}{\pi t}} \cos(t - \phi_k) \quad (\text{F8})$$

amounts to a good approximation at least for $t \gg |k^2 - 1/4|$ (see also below Eq. (58) in [46]), and

$$J_k(t) \simeq \sqrt{\frac{2}{\pi t}} \left[\cos(t - \phi_k) - \frac{4k^2 - 1}{8t} \sin(t - \phi_k) \right] \quad (\text{F9})$$

to an even better approximation at least for $t \gg |(k^2 - 1/4)(k^2 - 9/4)|$, and so on.

For an arbitrary but fixed t it is known (see (9.3.1) in [37]) that

$$J_k(t) \sim \frac{1}{\sqrt{2\pi k}} \left(\frac{et}{2k} \right)^k \text{ for } k \rightarrow \infty. \quad (\text{F10})$$

Finally, we derive yet another interesting property which seems not generally known. Focusing on $t \geq 0$ and observing that $(n+k)! \geq n!k!$ we can conclude from Eq. (F1) that

$$|J_k(t)| \leq \frac{(t/2)^k}{k!} D_k, \quad (\text{F11})$$

$$D_k := \sum_{n=0}^{\infty} \left(\frac{(t/2)^n}{n!} \right)^2. \quad (\text{F12})$$

Since any sum $\sum_{n=1}^N c_n$ with non-negative summands c_n satisfies the inequality $(\sum_{n=1}^N c_n)^2 \geq \sum_{n=1}^N c_n^2$ we obtain

$$D_k \leq \left(\sum_{n=0}^{\infty} \frac{(t/2)^n}{n!} \right)^2 = \left(e^{t/2} \right)^2 = e^t. \quad (\text{F13})$$

Moreover, $k!$ in Eq. (F11) can be lower bounded by $(k/e)^k$ according to some suitable version of Stirling's formula, yielding

$$|J_k(t)| \leq \left(\frac{te}{2k} \right)^k e^t = e^{t-kq}, \quad (\text{F14})$$

$$q := \ln k - \ln t + \ln 2 - 1. \quad (\text{F15})$$

Focusing on $t \leq k/2$ it follows that $\ln t \leq \ln k - \ln 2$, hence

$$q \geq 2 \ln 2 - 1 \geq 0.38. \quad (\text{F16})$$

For any given $a > 0$ we thus can conclude that

$$|J_k(t)| \leq e^{-a} \text{ if } t \leq 0.38k - a. \quad (\text{F17})$$

Note that our previous assumption $t \leq k/2$ is automatically fulfilled.

The main message of Eq. (F17) is that the Bessel functions $J_k(t)$ remain negligibly small up to times t which grow linearly with k . The quantitative numerical examples in Fig. 12 suggest that this seems indeed to be the

case up to times t close to k , i.e., the analytical upper bound in Eq. (F17) is still not very tight. Fig. 12 moreover suggests that this initial near-zero phase for $t < k$ directly goes over into damped oscillations for $t > k$, whose envelopes are right away in quite good agreement with those of the analytical long-time asymptotics from Eq. (F8), while the numerically observed frequencies of the oscillations remain notably slower than in Eq. (F8) up to considerably larger times, in agreement with the convergence criterion below Eq. (F8).

Appendix G: Derivation of Eq. (71)

Exploiting Eqs. (67)-(69) it follows that the integrand in Eq. (66),

$$I(x) := -\cos(kx) \tanh(\beta|J| \cos(x)/2) \exp\{it \cos(x)\}, \quad (\text{G1})$$

is an even and 2π -periodic function of x with the property $I(x + \pi) = -I^*(x)$. We thus can conclude from Eq. (66) that

$$\tilde{B}_0(t) = \int_{-\pi}^{\pi} dx \frac{I(x)}{2\pi} = \int_{-\pi/2}^{3\pi/2} dx \frac{I(x)}{2\pi} = \frac{K(t) + \tilde{K}(t)}{2\pi}, \quad (\text{G2})$$

$$K(t) := \int_{-\pi/2}^{\pi/2} dx I(x), \quad (\text{G3})$$

$$\tilde{K}(t) := \int_{-\pi/2}^{\pi/2} dx I(x + \pi) = -K^*(t), \quad (\text{G4})$$

implying

$$\text{Im}(\tilde{B}_0(t)) = \text{Im}(K(t))/\pi. \quad (\text{G5})$$

Next, we go over from the integration variable x in Eq. (G3) to $y := 2 \sin(x/2)$ (and we tacitly restrict ourselves to the integration domain on the right-hand side, i.e. to $x \in [-\pi/2, \pi/2]$). It follows that $dy/dx = \cos(x/2) = \sqrt{1 - \sin^2(x/2)}$, where we exploited that $\cos(x/2) \geq 0$ for all $x \in [-\pi/2, \pi/2]$. Hence, $dx = dy(1 - y^2/4)^{-1/2}$. Moreover $\cos(x) = 1 - 2 \sin^2(x/2) = 1 - y^2/2$. Altogether, we thus obtain

$$K(t) = \int_{-\sqrt{2}}^{\sqrt{2}} dy g(y) \exp\{it(1 - y^2/2)\}, \quad (\text{G6})$$

$$g(y) := \frac{-\tanh\{(\beta J/2)(1 - y^2/2)\}}{\sqrt{1 - y^2/4}}. \quad (\text{G7})$$

Note that $g(y)$ is an analytic function within the entire integration domain in Eq. (G6), i.e. for all $y \in [-\sqrt{2}, \sqrt{2}]$. (The singularities are at $y = \pm 2$.) Hence, $g(y)$ can be written for all $y \in [-\sqrt{2}, \sqrt{2}]$ as a convergent power series of the form

$$g(y) = \sum_{n=0}^{\infty} b_n y^{2n} \quad (\text{G8})$$

with real coefficients

$$b_0 = -\tanh(\beta J/2), \quad b_1 = \frac{b_0}{8} + \frac{\beta J}{4 \cosh(\beta J/2)}, \quad \dots \quad (\text{G9})$$

Accordingly, Eq. (G6) can be rewritten as

$$K(t) = \sum_{n=0}^{\infty} b_n c_n(t), \quad (\text{G10})$$

$$c_n(t) := \int_{-\sqrt{2}}^{\sqrt{2}} dy y^{2n} \exp\{it(1 - y^2/2)\}. \quad (\text{G11})$$

Upon partial integration one thus obtains the recursion relation

$$c_n(t) = \frac{i}{t} \left(2^{n+1/2} - (2n-1)c_{n-1}(t) \right). \quad (\text{G12})$$

Moreover, one can infer from Eq. (G11) that

$$c_0(t) = \sqrt{\frac{2}{t}} e^{it} h(\sqrt{t}), \quad (\text{G13})$$

$$h(t) := \int_{-t}^t dx e^{-ix^2}. \quad (\text{G14})$$

Defining the complex function

$$f(z) := e^{-z^2}, \quad (\text{G15})$$

which is analytical for all $z \in \mathbb{C}$, and the path in the complex plane

$$\gamma_1(s) := e^{i\pi/4}s \quad \text{with } s \in [-t, t], \quad (\text{G16})$$

we can rewrite Eq. (G14) as

$$h(t) = e^{-i\pi/4} \int_{\gamma_1} dz f(z). \quad (\text{G17})$$

Furthermore, standard arguments of complex analysis imply

$$\int_{\gamma_1} dz f(z) = \int_{\gamma_2} dz f(z) + \int_{\gamma_3} dz f(z) - \int_{\gamma_4} dz f(z), \quad (\text{G18})$$

where

$$\gamma_2(s) := s \quad \text{with } s \in [-t, t], \quad (\text{G19})$$

$$\gamma_3(s) := t e^{is} \quad \text{with } s \in [0, \pi/4], \quad (\text{G20})$$

$$\gamma_4(s) := t e^{is} \quad \text{with } s \in [\pi, \pi + \pi/4]. \quad (\text{G21})$$

For large t this implies the approximation

$$\int_{\gamma_2} dz f(z) = \sqrt{\pi} \quad (\text{G22})$$

up to corrections which are exponentially small in t . Finally, one finds that

$$\int_{\gamma_4} dz f(z) = - \int_{\gamma_3} dz f(z) \quad (\text{G23})$$

and that (see Appendix H for the details)

$$\int_{\gamma_3} dz f(z) = \frac{i}{2t} e^{i(\pi/4-t^2)} (1 + i/2t^2 + \mathcal{O}(t^{-4})) . \quad (\text{G24})$$

Altogether, we thus can conclude from Eqs. (G17), (G18), (G22)-(G24) that

$$h(t) = e^{-i\pi/4} \sqrt{\pi} + \frac{i}{t} e^{-it^2} (1 + i/2t^2 + \mathcal{O}(t^{-4})) \quad (\text{G25})$$

and with Eq. (G13) that

$$c_0(t) = \sqrt{\frac{2\pi}{t}} e^{i(t-\pi/4)} + i \frac{\sqrt{2}}{t} - \frac{1}{\sqrt{2}t^2} + \mathcal{O}(t^{-3}). \quad (\text{G26})$$

Furthermore, Eq. (G12) yields

$$c_1(t) = i \frac{2^{3/2}}{t} - i \sqrt{\frac{2\pi}{t^3}} e^{i(t-\pi/4)} + \frac{\sqrt{2}}{t^2} + \mathcal{O}(t^{-3}) \quad (\text{G27})$$

and (upon iteration of Eq. (G12))

$$c_n(t) = i \frac{2^{n+1/2}}{t} - \delta_{n,2} \frac{6}{t} \sqrt{\frac{2\pi}{t}} e^{i(t-\pi/4)} + \frac{2n-1}{t^2} 2^{n-1/2} + \mathcal{O}(t^{-3}) \quad \text{for } n \geq 2. \quad (\text{G28})$$

Introducing these results into Eq. (G10) yields

$$K(t) = \sqrt{\frac{2\pi}{t}} \left(b_0 - i \frac{b_1}{t} \right) e^{i(t-\pi/4)} + R(t) + \mathcal{O}(t^{-3}), \quad (\text{G29})$$

$$R(t) := i \frac{\sqrt{2}}{t} \sum_{n=0}^{\infty} b_n 2^n + \frac{1}{\sqrt{2}t^2} \sum_{n=0}^{\infty} b_n (2n-1) 2^n . \quad (\text{G30})$$

Observing Eq. (G8), the first sum in Eq. (G30) can be identified with $g(\sqrt{2})$, and hence with zero according to Eq. (G7). Likewise, in the second sum in Eq. (G30) we can replace $(2n-1)$ by $2n$, yielding

$$R(t) = \frac{2^{3/2}}{t^2} \sum_{n=0}^{\infty} b_n n 2^{n-1} = \frac{2^{3/2}}{t^2} g'(\sqrt{2}) = \frac{2^{3/2} \beta J}{t^2}. \quad (\text{G31})$$

By exploiting Eqs. (G29) and (G31) in (G5) we obtain

$$\begin{aligned} \text{Im}(\tilde{B}_0(t)) &= \sqrt{\frac{2}{\pi t}} b_0 \sin(t - \pi/4) \\ &- \sqrt{\frac{2}{\pi t^3}} b_1 \cos(t - \pi/4) + \mathcal{O}(t^{-3}). \end{aligned} \quad (\text{G32})$$

Introducing this result and the large- t asymptotics for $J_0(t)$ from Eq. (F8) into Eq. (70) yields Eq. (71) in the main text.

Appendix H: Derivation of Eq. (G24)

Exploiting Eqs. (G15) and (G20) yields

$$\int_{\gamma_3} dz f(z) = \int_0^{\pi/4} ds it e^{is} e^{-t^2 e^{2is}} . \quad (\text{H1})$$

Employing $x := \pi/2 - 2s$ as new integration variable one finds that

$$\int_{\gamma_3} dz f(z) = \frac{i}{2t} e^{i(\pi/4-t^2)} I(t) , \quad (\text{H2})$$

$$\begin{aligned} I(t) &:= t^2 \int_0^{\pi/2} dx e^{-ix/2} e^{-t^2(e^{i(\pi/2-x)} - i)} \\ &= t^2 \int_0^{\pi/2} dx e^{-ix/2} e^{-it^2(\cos(x)-1)} e^{-t^2 \sin(x)} . \end{aligned} \quad (\text{H3})$$

For large values of t , the last factor implies that the integral is dominated by small values of x . Rewriting $\cos(x)$ and $\sin(x)$ as power series and employing $y := t^2 x$ as new integration variable then yields $I(t) = 1 + i/2t^2 + \mathcal{O}(t^{-4})$. Together with Eq. (H2) we thus recover Eq. (G24).

Appendix I: Counterpart of Eq. (86) for $V = s_\nu^y$

Our objective is to show that the counterpart of the approximation (86) for perturbations $V = s_\nu^y$ instead of $V = s_\nu^x$ is given by

$$\langle s_\alpha^x \rangle_t - \langle s_\alpha^x \rangle_{\text{th}} = \delta_{\nu\alpha} \frac{g\beta}{4} \sin(Gt) e^{-\omega^2 t^2/4} . \quad (\text{I1})$$

According to the assumptions above Eq. (86), only the first summand with $k = 0$ has to be kept in Eq. (14). In view of Eq. (13), the approximation (86) is therefore equivalent to

$$C_x(t) = f(t) \cos(Gt) \quad (\text{I2})$$

with the abbreviations

$$C_x(t) := C_{s_\nu^y s_\alpha^x}(t) , \quad (\text{I3})$$

$$f(t) := \delta_{\nu\alpha} \frac{g\beta}{4} e^{-\omega^2 t^2/4} , \quad (\text{I4})$$

where the dependence of $C_x(t)$ and $f(t)$ on ν and α has been omitted. Likewise, Eq. (I1) is equivalent to

$$C_{s_\nu^y s_\alpha^x}(t) = f(t) \sin(Gt) . \quad (\text{I5})$$

For symmetry reasons (see also above Eq. (78)), this relation is in turn equivalent to

$$C_y(t) = -f(t) \sin(Gt) , \quad (\text{I6})$$

where

$$C_y(t) := C_{s_\nu^x s_\alpha^y}(t) . \quad (\text{I7})$$

In summary, Eq. (I2) is considered as given and Eq. (I6) as to be shown.

Similarly as in Eq. (7), we define

$$H' := H + GS^z , \quad (\text{I8})$$

where

$$S^z := \sum_{l=1}^L s_l^z . \quad (\text{I9})$$

In other words, H' is given by the right-hand side of Eq. (7) with $G = 0$. In the same way, ρ'_{can} is obtained by replacing H by H' in Eq. (5), and analogously for $A'(t)$ in Eq. (11), A'_{th} in Eq. (12), and $C'_{VA}(t)$ in Eq. (13). Finally, Eq. (B43) together with Eqs. (11)-(13) implies that Eqs. (I2), (I3) can be rewritten as

$$C_x(t) = \text{tr}\{\rho_{can} s_\nu^x e^{iHt} s_\alpha^x e^{-iHt}\} = f(t) \cos(Gt) . (\text{I10})$$

Similarly, it follows by recalling that H' amounts to the case $G = 0$ (see below Eq. (I9)) that

$$\text{tr}\{\rho'_{can} s_\nu^x e^{iH't} s_\alpha^x e^{-iH't}\} = f(t) , \quad (\text{I11})$$

while Eq. (I7) can now be rewritten as

$$C_y(t) = \text{tr}\{\rho_{can} s_\nu^x e^{iHt} s_\alpha^y e^{-iHt}\} . \quad (\text{I12})$$

As mentioned above Eq. (8) and below Eq. (A1), S^z commutes with H , implying together with Eq. (I8) that $e^{iH't} = e^{iHt} e^{iGs^z t}$. Moreover, all summands s_l^z in Eq. (I9) commute with each other, and all s_l^z with $l \neq \alpha$ commute with s_α^x , as detailed above Eq. (A2). We thus

can conclude that

$$e^{iH't} s_\alpha^x e^{-iH't} = e^{iHt} B_t e^{-iHt} , \quad (\text{I13})$$

$$B_t := e^{iGs_\alpha^z t} s_\alpha^x e^{-iGs_\alpha^z t} . \quad (\text{I14})$$

Working in terms of Pauli matrices (see above Eq. (A2)), a straightforward calculation then yields

$$B_t = s_\alpha^x \cos(Gt) - s_\alpha^y \sin(Gt) . \quad (\text{I15})$$

Let us now assume that ρ'_{can} in Eq. (I11) can be approximately replaced by ρ_{can} . One thus can conclude from Eqs. (I10)-(I15) that

$$f(t) \cos^2(Gt) - \sin(Gt) C_y(t) = f(t) \quad (\text{I16})$$

One readily sees that Eq. (I6) is the unique solution of this equation for all t with $\sin(Gt) \neq 0$. For the remaining t 's, the same result (I6) follows under the physically obvious extra assumption that $C_y(t)$ must be a continuous function of t . In other words, in order to accomplish our goal of validating Eq. (I6), we are left to justify our approximation of ρ'_{can} in Eq. (I11) by ρ_{can} . Generally speaking, it seems reasonable to expect that this may actually be impossible. On the other hand, for $\beta \rightarrow 0$ it is quite obvious that $\rho'_{can} = \rho_{can}$, hence our approximation can be justified at least for sufficiently small β . Since the same has already been taken for granted above Eq. (86), and therefore also in Eqs. (I1) and (I6), this argument is sufficient for our present purposes.

-
- [1] C. Gogolin and J. Eisert, Equilibration, thermalization, and the emergence of statistical mechanics in closed quantum systems, Rep. Prog. Phys. **79**, 056001 (2016).
 - [2] L. D'Alessio, Y. Kafri, A. Polkovnikov, and M. Rigol, From Quantum Chaos and Eigenstate Thermalization to Statistical Mechanics and Thermodynamics, Adv. Phys. **65**, 239 (2016).
 - [3] T. Mori, T. N. Ikeda, E. Kaminishi, and M. Ueda, Thermalization and prethermalization in isolated quantum systems: a theoretical overview, J. Phys. B **51**, 112001 (2018).
 - [4] M. Ueda, Quantum equilibration, thermalization and prethermalization in ultracold atoms, Nat. Rev. Phys. **2**, 669 (2020).
 - [5] N. Shiraishi and H. Tasaki, Nature abhors a vacuum: A simple rigorous example of thermalization in an isolated macroscopic quantum system, J. Stat. Phys. **191**, 82 (2024).
 - [6] H. Tasaki, Macroscopic Irreversibility in Quantum Systems: ETH and Equilibration in a Free Fermion Chain, arXiv:2401.15263
 - [7] H. Tasaki, Heat flows from hot to cold: A simple rigorous example of thermalization in an isolated macroscopic quantum system, arXiv:2404.04533
 - [8] B. Roos, S. Teufel, R. Tumulka, and C. Vogel, Macroscopic Thermalization for Highly Degenerate Hamiltonians, arXiv:2408.15832
 - [9] P. Reimann and C. Eidecker-Dunkel, Onsager's regression hypothesis adjusted to quantum systems, Phys. Rev. B **110**, 014306 (2024).
 - [10] P. Reimann, Foundation of statistical mechanics under experimentally realistic conditions, Phys. Rev. Lett. **101**, 190403 (2008).
 - [11] N. Linden, S. Popescu, A. J. Short, and A. Winter, Quantum mechanical evolution towards equilibrium, Phys. Rev. E **79**, 061103 (2009).
 - [12] A. J. Short, Equilibration of quantum systems and subsystems, New J. Phys. **13**, 053009 (2011).
 - [13] P. Reimann and M. Kastner, Equilibration of macroscopic quantum systems, New J. Phys. **14**, 043020 (2012).
 - [14] A. J. Short and T. C. Farrelly, Quantum equilibration in finite time, New J. Phys. **14**, 013063 (2012).
 - [15] B. N. Balz and P. Reimann, Equilibration of isolated many-body quantum systems with respect to general distinguishability measures, Phys. Rev. E **93**, 062107 (2016).
 - [16] J. von Neumann, Beweis des Ergodensatzes und des H-Theorems in der neuen Mechanik, Z. Phys. **57**, 30 (1929) [English translation by R. Tumulka, Proof of the ergodic theorem and the H-theorem in quantum mechanics, Eur. Phys. J. H **35**, 201 (2010)].
 - [17] J. M. Deutsch, Quantum statistical mechanics in a closed system, Phys. Rev. A **43**, 2046 (1991).
 - [18] M. Srednicki, Chaos and quantum thermalization, Phys.

- Rev. E **50**, 888 (1994).
- [19] M. Rigol, V. Dunjko, and M. Olshanii, Thermalization and its mechanism for generic isolated quantum systems, *Nature* **452**, 854 (2008).
- [20] T. Farrelly, F. G. S. L. Brandão, and M. Cramer, Thermalization and return to equilibrium on finite quantum lattice systems, *Phys. Rev. Lett.* **118**, 140601 (2017).
- [21] L. Dabelow, P. Vorndamme, and P. Reimann, Thermalization of locally perturbed many-body quantum systems, *Phys. Rev. B* **105**, 024310 (2022).
- [22] E. Barouch, B. M. McCoy, and M. Dresden, Statistical Mechanics of the XY Model. I, *Phys. Rev. A* **2**, 1075 (1970); E. Barouch and B. M. McCoy, Statistical Mechanics of the XY Model. III, *Phys. Rev. A* **3**, 2137 (1971).
- [23] See around Eq. (5) in Ref. [6].
- [24] H. Touchette, Equivalence and nonequivalence of ensembles: thermodynamic, macrostate, and measure levels, *J. Stat. Phys.* **159**, 987 (2015).
- [25] F. G. S. L. Brandao and M. Cramer, Equivalence of Statistical Mechanical Ensembles for Non-Critical Quantum Systems, arXiv:1502.03263
- [26] H. Tasaki, On the local equivalence between the canonical and the microcanonical ensembles for quantum spin systems, *J. Stat. Phys.* **172**, 905 (2018).
- [27] T. Kuwahara and K. Saito, Gaussian concentration bound and ensemble equivalence in generic quantum many-body systems including long-range interactions, *Ann. Phys.* **421**, 168278 (2020).
- [28] H. Spohn, Interacting and noninteracting integrable systems, *J. Math. Phys.* **59**, 091402 (2018).
- [29] This symmetry property can be verified by similar calculations as in the Supplementary Sec. I.D of Ref. [36]. However, it also appears to us intuitively quite obvious, hence we omit here those quite lengthy calculations.
- [30] E. H. Lieb and D. W. Robinson, The finite group velocity of quantum spin systems, *Commun. Math. Phys.* **28**, 251 (1972).
- [31] J. Stolze, A. Nöppert, and G. Müller, Gaussian, exponential, and power-law decay of time-dependent correlation functions in quantum spin chains, *Phys. Rev. B* **52**, 4319 (1995).
- [32] S. Bravyi, M. B. Hastings, and F. Verstraete, Lieb-Robinson bounds and the generation of correlations and topological quantum order, *Phys. Rev. Lett.* **97**, 050401 (2006).
- [33] F. H. L. Essler and M. Fagotti, Quench dynamics and relaxation in isolated integrable quantum spin chains, *J. Stat. Mech.* **6**, 064002 (2016).
- [34] C. Duval and M. Kastner, Quantum kinetic perturbation theory for near-integrable spin chains with weak long-range interactions, *New J. Phys.* **21**, 093021 (2019).
- [35] A. R. Its, A. G. Izergin, V. E. Korepin, and N. A. Slavnov, Temporal correlations of quantum spins, *Phys. Rev. Lett* **70**, 1704 (1993).
- [36] C. Eidecker-Dunkel and P. Reimann, Allosteric impurity effects in long spin chains, *Phys. Rev. B* **108**, 054407 (2023).
- [37] M. Abramowitz and A. Stegun, *Handbook of Mathematical Functions*, Dover 1972.
- [38] The “+1” on the left-hand side of Eq. (57) is needed to guarantee $L \gg 1$ even if $\nu = \alpha$.
- [39] H. B. Cruz and L. L. Goncalves, Time-dependent correlations of the one-dimensional isotropic XY model, *J. Phys. C: Solid State Phys.* **14**, 2785 (1981).
- [40] J. Stolze, V. S. Viswanath, and G. Müller, Dynamics of semi-infinite quantum spin chains at $T = \infty$, *Z. Phys. B* **89**, 45 (1992).
- [41] O. Derzhko, T. Krokhmalskii, and J. Stolze, Dynamics of the spin-1/2 isotropic XY chain in a transverse field, *J. Phys. A: Math. Gen.* **33**, 3063 (2000).
- [42] E. Lieb, T. Schultz, and D. Mattis, Two Soluble Models of an Antiferromagnetic Chain, *Ann. Phys.* **16**, 407 (1961).
- [43] M. Gluza, J. Eisert, and T. Farrelly, Equilibration towards generalized Gibbs ensembles in non-interacting theories, *SciPost Phys.* **7**, 038 (2019).
- [44] C. Murthy and M. Srednicki, Relaxation to Gaussian and generalized Gibbs states in systems of particles with quadratic Hamiltonians, *Phys. Rev. E* **100**, 012146 (2019).
- [45] Viewing a “model” as being defined by a Hamiltonian H and an initial state $\rho(0)$, a statistical ensemble of models is usually generated by randomizing either H or $\rho(0)$ in some suitable way.
- [46] mathworld.wolfram.com/BesselFunctionoftheFirstKind.html